Reports of the Department of Geodetic Science

Report No. 288

GLOBAL ACCURACY ESTIMATES OF POINT AND MEAN UNDULATION DIFFERENCES OBTAINED FROM GRAVITY DISTURBANCES, GRAVITY ANOMALIES AND POTENTIAL COEFFICIENTS

by

Christopher Jekeli

Prepared for

National Aeronautics and Space Administration
Goddard Space Flight Center
Greenbelt, Maryland 20771

Grant NGR 36-008-161

The Ohio State University
Department of Geodetic Science
1958 Neil Avenue
Columbus, Ohio 43210

Abstract

Through the method of truncation functions, the oceanic geoid undulation is divided into two constituents: an inner zone contribution expressed as an integral of surface gravity disturbances over a spherical cap, and an outer zone contribution derived from a finite set of potential harmonic coefficients. Global, average error estimates are formulated for undulation differences, thereby providing accuracies for a relative geoid. The error analysis focuses on the outer zone contribution for which the potential coefficient errors are modeled on the assumption that the coefficients are determined from a global distribution of $1^\circ \times 1^\circ$ mean anomalies. The method of computing undulations based on gravity disturbance data for the inner zone is compared to the similar, conventional method which presupposes gravity anomaly data within this zone. The two methods exhibit analogous error characteristics, the estimated errors of the gravity disturbance method being only slightly better. For continuous and errorless gravity data inside a spherical cap having a radius of 10° and with potential coefficients derived to degree 180 from a global set of $1^\circ \times 1^\circ$ mean anomalies given to an accuracy of ± 10 mgal (± 1 mgal), the typical error in the difference of undulations is 30 cm to 40 cm (5 cm to 10 cm), depending on their separation. In the absence of more detailed cap data, the error is as high as 160 cm (70 cm). In the latter case, the corresponding error for $1^\circ \times 1^\circ$ mean undulation differences is about 140 cm (30 cm).

Foreword

This report was prepared by Mr. Christopher Jekeli, Graduate Research Associate, Department of Geodetic Science, The Ohio State University. This work was supported under NASA Grant NGR 36-008-161, The Ohio State University Research Foundation Project No. 783210, Project Supervisor, Richard H. Rapp. The grant covering this research is administered through the NASA Goddard Space Flight Center, Greenbelt, Maryland, Mr. James Marsh, Technical Officer.

The support and guidance provided by my advisor, Dr. Richard H. Rapp, in all aspects of this report was deeply appreciated.

Table of Contents

1. Introduction

This report again attacks the problem of determining the geoid accurately from gravity information over the entire globe. The route that is normally followed starts with a formulation of the geoid undulation in terms of mean gravity anomalies, or potential harmonic coefficients, or both and follows with an examination of how the errors in these observed quantities propagate into the computed undulation; see for example, Rapp and Rummel (1975) and Christodoulidis (1976), to mention only two.

Christodoulidis based his thorough error analysis on the method by which undulations are computed from mean gravity anomalies and a set of potential coefficients (according to Molodenskii's truncation theory). Moritz (1974) outlined a procedure in which the undulations are determined not by integrating gravity anomalies (Stokes' formula), but by integrating gravity disturbances. It is the purpose of this report to carry out an error analysis of undulations (more precisely, undulation differences) that are also obtained according to Molodenskii's truncation theory, but as applied to an integral of gravity disturbances. The structure of the analysis is very similar to that of Christodoulidis. From his conclusions, it is evident that the procurement of a highly accurate ($\sim$ 10 cm) relative geoid on the oceans requires a dense and accurate network of gravity anomalies around each point of computation, as well as potential coefficients to at least degree 70. We shall see that the method of determining the geoid from gravity disturbance data under most practical circumstances can claim little, if any, substantial improvement in accuracy over the conventional method. Because the ultimate determination of the sea surface topography is foreseen to be effected by combining accurate geoid undulations and satellite altimetry, the areas of primary interest are the oceans. Therefore, this alternate method does offer two advantages; first, measured gravity values on the ocean's surface need not be reduced to the geoid (which differs from the surface of the ocean by the "sea surface topography," on the order of 1 m), and secondly, satellite altimetry as additional observed data fits very neatly into the process.

For reasons to be explained later, the analysis here is essentially devoted to investigating the effects on the undulation due to erroneous potential coefficients, as well as the lack of higher-degree coefficients. The discussion is further limited to the case in which the earth is approximated by a sphere. Moritz (1974) treats the effect of the earth's ellipticity; Christodoulidis (1976) thoroughly studied the corrections for the atmosphere which are applicable also in this case; and finally, the terrain correction is negligibly small on the oceans.

2. The Concept in Principle

The known orbit of a satellite determines its altitude above the reference ellipsoid. The altimeter measurement a establishes the sea surface height h above the ellipsoid (see Figure 1). This height is the sum of the geoid undu-

lation N and the sea surface topography t, since it is generally assumed that the three surfaces depicted in the figure are parallel locally.

Figure 1.

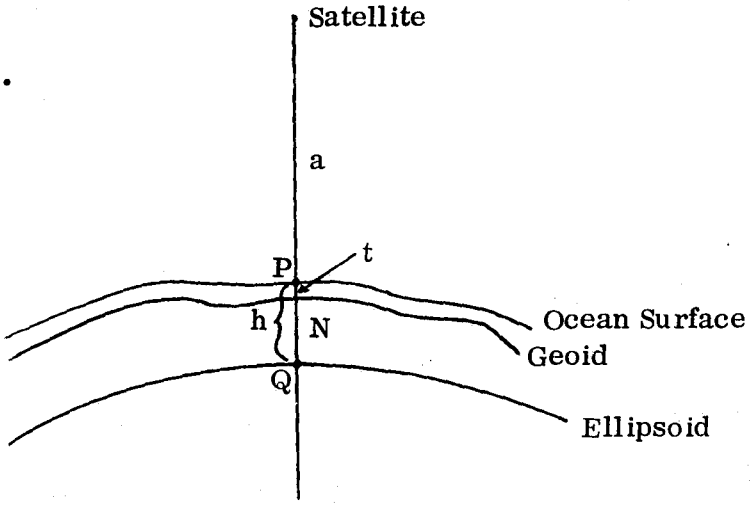

Gravity g is measured on the sea surface, e.g. at point P, while the normal gravity γ_P at P is computed with the aid of the sea surface height:

$$\gamma_P = \gamma_Q + \frac{\partial \gamma}{\partial h}\bigg|_Q h \qquad (1)$$

where the normal gravity γ_Q on the ellipsoid and its radial derivative are known quantities. Thus, the sea surface height as obtained from the altimeter measurement serves the dual purpose of providing normal gravity at P, as well as the sea surface topography for a known undulation.

We note that the gravity measurements on the surface could be reduced to the geoid if the heights of the sea surface above the geoid were known; but precisely these heights are to be determined. Therefore, in practice it is simpler conceptually to obtain gravity disturbances (aided by altimetry data) on the ocean surface, than gravity anomalies on the geoid, the latter being required for any use of Stokes' formula.

From the definition of the gravity disturbance, $\delta g = g_P - \gamma_P$, and the disturbing potential T, there is the basic relation (Heiskanen and Moritz 1967, p. 85):

$$\delta g = -\frac{\partial T}{\partial h} \qquad (2)$$

From this and with a spherical approximation, Moritz (1974) derives

$$T = \frac{R}{4\pi} \int_\sigma \int \delta g \; \bar{S}(\psi) \, d\sigma \qquad (3)$$

where σ is the unit sphere, and δg is given everywhere on the earth's surface (assumed to be a sphere of radius R). $\bar{S}(\psi)$ is an analogue to Stokes' function, defined by

$$\bar{S}(\psi) = \sum_{n=0}^{\infty} \frac{2n+1}{n+1} P_n(\cos\psi) = \csc\frac{\psi}{2} - \ell n\left(1+\csc\frac{\psi}{2}\right) \qquad (4)$$

The argument ψ is the usual central angle between the point at which T is computed (on the sea surface) and the surface element $d\sigma$. The closed expression for the infinite sum is derived by Hotine (1969, p. 311). Note that the sum in (4) includes zero- and first-degree harmonics; whereas, these are absent in Stokes' function.

Let γ be the normal gravity in the ellipsoid. The difference between the disturbing potential on the geoid, $T = N\gamma$ (Bruns' formula), and the disturbing potential on the sea surface (equ. (3)) is approximately $t\,\delta g$ and is neglected (for $t = 2$ m, $\delta g = 40$ mgal, $N = 30$ m, it is only .003% of T). Hence, the geoid undulation in terms of gravity disturbances is

$$N = \frac{R}{4\pi\gamma} \iint_{\sigma} \delta g\, \bar{S}(\psi)\, d\sigma \qquad (5)$$

It is mentioned again that this, as Stokes' integral, is only a spherical approximation, so that γ becomes an average value of normal gravity.

The integral in (5) is unlike the usual Stokes' integral, however, in that it incorporates the zero-degree and first-degree potential harmonics. Whereas, the gravity anomalies in Stokes' integral must average to zero (so that N is the geoid undulation with respect to the given reference ellipsoid) and have no first-degree term in their harmonic expansion, no such provisions are necessary for the gravity disturbances in (3) or (5) (see also Hotine 1969, p. 317). Nevertheless, since the error analysis will require a decomposition of the undulation N into spherical harmonics, the zero-degree and first-degree contributions will be singled out. Certainly, if the global gravity disturbance data are known to possess neither zero- nor first-degree harmonics, then $\bar{S}(\psi)$ could be modified by also excluding its first two harmonics (see the end of section 3 and Appendix C).

3. Truncation Coefficients

To compute the undulation from an integral equation such as (5), gravity must be known, in theory, at every point on the earth. In practice, of course, such detailed gravity information is not attainable. Instead, only a finite set of measurements is available in the vicinity of the point of computation. Limiting the integration in (5) to this area is not sufficient, however, since geoid undulations are predominantly the consequence of the global features of the gravity field (as, for example, an inspection of the degree variances of the undulation covariance function shows). Therefore, the influence of the "remote zones" must be taken into account, and this is usually accomplished by separating the contributions of the inner and outer zones as follows:

$$N = \frac{R}{4\pi\gamma}\int\int_{\sigma_c} \delta g\, \bar{S}(\psi)\, d\sigma + \frac{R}{4\pi\gamma}\int\int_{\sigma-\sigma_c} \delta g\, \bar{S}(\psi)\, d\sigma \qquad (6)$$

$$= \qquad N_1 \qquad + \qquad N_2 \qquad (7)$$

where σ_c is a spherical cap with radius ψ_o, $\sigma - \sigma_c$ being the "cap" with radius $\pi - \psi_o$. The evaluation of N_2 is predicated on a given set of potential harmonic coefficients, and therefore, should be rewritten in the form of an infinite series. A way to proceed follows the lines of development given by Heiskanen and Moritz (1967), sec. 7.4, starting with the definition

$$\bar{S}_1(\psi) = \begin{cases} 0, & \text{if } 0 < \psi < \psi_o \\ \bar{S}(\psi), & \text{if } \psi_o \le \psi < \pi \end{cases} \qquad (8)$$

$\bar{S}_1(\psi)$ is piecewise continuous in the interval $0 < \psi < \pi$, and hence, this function is expandable in a series of Legendre polynomials:

$$\bar{S}_1(\psi) = \sum_{n=0}^{\infty} k_n \bar{Q}_n P_n(\cos\psi) \qquad (9)$$

The coefficients $k_n Q_n$ are determined by multiplying both sides of equation (9) by $P_n(\cos\psi)$ and integrating over $0 < \psi < \pi$ (taking advantage of the orthogonality of P_n):

$$k_n \bar{Q}_n = \frac{2n+1}{2}\int_0^{\pi} \bar{S}_1(\psi)\, P_n(\cos\psi)\, \sin\psi\, d\psi \qquad (10)$$

With the choice

$$k_n = \frac{2n+1}{2}$$

equation (10) becomes, upon substituting (8),

$$\bar{Q}_n(\psi_o) = \int_{\psi_o}^{\pi} \bar{S}(\psi)\, P_n(\cos\psi)\, \sin\psi\, d\psi \qquad (11)$$

Let coordinates (ψ, α) be spherical coordinates on a sphere where the pole is the point (θ, λ) at which N is to be computed. Then, from (6) and (7),

$$N_2 = \frac{R}{4\pi\gamma}\int_0^{2\pi}\int_{\psi_o}^{\pi} \delta g(\psi,\alpha)\, \bar{S}(\psi)\, \sin\psi\, d\psi\, d\alpha \qquad (12)$$

which in view of (8) and (9) is

$$N_2 = \frac{R}{4\pi\gamma}\sum_{n=0}^{\infty}\frac{2n+1}{2}\bar{Q}_n\int_0^{2\pi}\int_0^{\pi} \delta g(\psi,\alpha)\, P_n(\cos\psi)\sin\psi\, d\psi\, d\alpha \qquad (13)$$

The gravity disturbance can also be expanded in a series of Laplace harmonics

(let θ, λ be the spherical coordinates of the point at which N_2 is computed):

$$\delta g(\theta,\lambda) = \sum_{n=0}^{\infty} \delta g_n(\theta,\lambda) \tag{14}$$

These Laplace harmonics, conversely, can be found by integrating the gravity distrubances (let (θ,λ) be the pole of the earth and use equ. (1-71) of Heiskanen and Moritz 1967):

$$\delta g_n(\theta,\lambda) = \frac{2n+1}{4\pi} \int_0^{2\pi}\int_0^{\pi} \delta g(\psi,\alpha) P_n(\cos\psi) \sin\psi \, d\psi \, d\alpha \tag{15}$$

A comparison of equations (15) and (13) shows that

$$N_2 = \frac{R}{2\gamma} \sum_{n=0}^{\infty} \bar{Q}_n \, \delta g_n \tag{16}$$

To achieve the objective of expanding N_2 in a series of potential coefficients, we write

$$\left.\begin{aligned} T &= \sum_{n=0}^{\infty} T_n \\ \text{with } T_n &= \frac{kM}{R} \sum_{m=0}^{n} [\, \bar{C}_{nm} \cos m\lambda + \bar{S}_{nm} \sin m\lambda \,]\, \bar{P}_{nm}(\cos\theta) \end{aligned}\right\} \tag{17}$$

$\bar{P}_{nm}(\cos\theta)$ is a fully normalized Legendre function; $\bar{C}_{nm}$, $\bar{S}_{nm}$ are fully normalized potential coefficients, with $\bar{C}_{nm}$ being the coefficients after the normal gravity field has been removed; and kM is the product of the gravitational constant and the mass of the earth. Finally, with (Moritz 1974, p. 48)

$$\delta g_n = \frac{n+1}{R} T_n \qquad \text{and} \qquad \gamma = \frac{kM}{R^2} \tag{18}$$

equation (16) becomes

$$N_2(\theta,\lambda) = \frac{R}{2} \sum_{n=0}^{\infty} (n+1) \bar{Q}_n \sum_{m=0}^{n} [\, \bar{C}_{nm} \cos m\lambda + \bar{S}_{nm} \sin m\lambda \,]\, \bar{P}_{nm}(\cos\theta) \tag{19}$$

Remembering that $\bar{Q}_n$ is a function of the cap radius ψ_0, it is noted that for $\psi_0 = 0$, $N_2 = N$. For $\psi_0 > 0$, the coefficients $\bar{Q}_n$, which are analogous to Molodenskii's truncation coefficients (Molodenskii, et al. 1962, p. 147), actually effect an increase in the rate of convergence of this series, as the contribution of the finer structure of the gravity field (the high-degree harmonics) is essentially accounted for by N_1 in equation (7). Of course, this increase in the convergence rate depends on the size of ψ_0.

The difference between Stokes' integral and its analogue in terms of gravity disturbances (equation (5)) has already been elucidated in the previous section. This difference has a direct bearing on the truncation coefficients $\bar{Q}_n$.

It is again noted that as opposed to Stokes' function the series expansion of $\bar{S}(\psi)$ (equation (4)) includes zero- and first-degree terms. If δg_o and δg_1 in the series expansion of δg (equation (14)) were zero, then the integral formula (5) in concept would not change; but in order to be consistent with Stokes' integral, the first two harmonics of $\bar{S}(\psi)$ could be excluded. This modification of the kernel function evidently induces a change in the truncation coefficients $\bar{Q}_n$ (see also section 10). Since the formulation of the truncation coefficients as presented above yields the higher error estimates in the analyses of section 7 (see also DeWitte 1966), the alternative approach using the modified kernel function $\bar{S}^*(\psi) = \bar{S}(\psi) - 1 - \frac{3}{2}\cos\psi$ is pursued only in Appendix C.

4. The Evaluation of $\bar{Q}_n$

There exists a handful of methods to evaluate the coefficients $\bar{Q}_n$; not all are equally accurate and efficient. Direct integration by analytic means seems plausible for small n (as Molodenskii has done for his coefficients). A recourse to numerical integration for larger n is unsatisfactory in view of the limited attainable accuracy and the singularity of $\bar{S}(\psi)$ at $\psi = 0$ (see equation (4)). It is possible also to determine a finite sum for each $\bar{Q}_n$ since P_n is expressible in this way. But the volume of computations (coupled with a loss of accuracy) for large n is prohibitive. A desirable formula for $\bar{Q}_n$ would be in the form of a recurrence relationship, such as Paul (1973) has derived for Molodenskii's coefficients by utilizing the series expansion of Stokes' function (Hagiwara (1976) also formulated a very elegant recursive solution).

In the case of the coefficients $\bar{Q}_n$, the integral (11) actually admits to a simplifying integration by parts, and by borrowing several results from Hagiwara (1976), a relatively simple recurrence formula can be derived. The appendix gives a full account of this derivation for $\psi_o \neq 0$. This solution of $\bar{Q}_n$ seems to yield quite accurate and very efficient evaluations even for small values of ψ_o. Although $\bar{S}(\psi_o)$ has a singularity at $\psi_o = 0$, $\bar{Q}_n$ is nevertheless well-defined there; for indeed, a comparison of (9) and (4) shows (noting that when $\psi_o = 0$, $\bar{S}(\psi) = \bar{S}_1(\psi)$ for $0 < \psi < \pi$)

$$\bar{Q}_n(0) = \frac{2}{n+1}, \qquad n \geq 0 \tag{20}$$

5. The Global Error Estimates

The total geoid undulation at a point can be expressed as an infinite series of spherical harmonics by combining Bruns' formula ($N = T/\gamma$), and equations (17) and (18):

$$N = \frac{R}{\gamma}\sum_{n=0}^{\infty}\frac{\delta g_n}{n+1} \tag{21}$$

Considering equations (7) and (16), (21) may be divided as follows:

$$
\left.
\begin{aligned}
N &= N_1 + N_2 \\
N_1 &= \frac{R}{\gamma} \sum_{n=0}^{\infty} \left(\frac{1}{n+1} - \frac{1}{2} \bar{Q}_n \right) \delta g_n \\
N_2 &= \frac{R}{2\gamma} [\bar{Q}_0 \, \delta g_0 + \bar{Q}_1 \, \delta g_1] + \frac{R}{2\gamma} \sum_{n=2}^{\infty} \bar{Q}_n \, \delta g_n
\end{aligned}
\right\} \quad (22)
$$

It is usual to assume in gravimetric determinations of the geoid that the centers of mass of the reference ellipsoid and the earth coincide. Then $\delta g_1 = 0$. However, their total masses may not be equal; in this case, the zero-degree term does not vanish and from (18) and Heiskanen and Moritz (1967, p. 98)

$$
\frac{R}{2\gamma} \bar{Q}_0 \, \delta g_0 = \frac{R}{2\gamma} \bar{Q}_0 \frac{T_0}{R} = \frac{\bar{Q}_0 \, k \, \delta M}{2\gamma R} \quad (23)
$$

where δM is the difference in the total masses. N_1 also contains a zero-degree term, but it is not necessary to treat it separately if N_1 is evaluated according to the integral expression of equation (6). To be observed is that the difference, δW, between the ellipsoidal and geoidal potentials has so far been ignored. If $\delta W \neq 0$, then by the generalized Bruns' formula ($N = (T - \delta W)/\gamma$) the total constant part of N is $k \delta M / \gamma R - \delta W / \gamma$.

The first infinite sum in (22) is the contribution to N from the gravity field within the cap σ_c (see equ. (6)). To obtain a high degree of accuracy in N_1 , one usually visualizes a sufficiently dense set of measured gravity and altimetry values in σ_c which are then processed in some systematic fashion resulting in an approximation to the first integral of (6). The errors in this approximation arise from errors in the gravity and altimetry data itself (propagated error), as well as from an unavailability of continuous data over the cap (discretion error). Christodoulidis (1976) investigated two methods which could provide estimates for the errors in N_1 when it is formulated (analogous to equ. (6)) as an integral of gravity anomalies. He concluded that these methods are computationally unfeasible and proceeded to estimate the corresponding errors in the so-called "frequency domain", that is, when N_1 is expressed in a spectral representation as in equation (22). The structural differences between the formulations of the geoid undulation in terms of gravity anomalies and in terms of gravity disturbances are practically nonexistent; and hence, it will be assumed that in the present context, the same type of numerical difficulties would occur in the error estimation of N_1 . Moreover, and for the same reason, it is obvious that a similar procedure as developed by Christodoulidis can lead to error estimates for N_1 in the frequency domain. Relying on the argument that the local behaviors of gravity anomalies and gravity disturbances are not inherently dissimilar, the derivations and evaluations of these error estimates are omitted with the assumption that no significant deviations from Christodoulidis' numerical results would be expected.

To put some rigor into the underlying argument, we digress briefly and derive the covariance function for gravity disturbances. For the disturbing potential, the covariance function is given by (Moritz 1972)

$$K(P,Q) = \sum_{n=2}^{\infty} \frac{R^2}{(n-1)^2} c_n \left(\frac{R^2}{r_P r_Q}\right)^{n+1} P_n(\cos\psi) \qquad (24)$$

where ψ is the spherical distance between the points P and Q , r_P , r_Q are the radius vectors to P and Q , and the c_n are the degree variances for gravity anomalies. By the law of propagation of covariances (Moritz 1972) as applied to the relation (2), the covariance function for gravity disturbances is

$$D(P,Q) = -\frac{\partial}{\partial r_P}\left[-\frac{\partial}{\partial r_Q} K(P,Q)\right] = \sum_{n=2}^{\infty} \left(\frac{n+1}{n-1}\right)^2 c_n \left(\frac{R^2}{r_P r_Q}\right)^{n+2} P_n(\cos\psi) \qquad (25)$$

By inspection, the degree variances for gravity disturbances are

$$d_n = \left(\frac{n+1}{n-1}\right)^2 c_n \ , \qquad n \geq 2 \qquad (26)$$

For large n , that is, for high frequencies, the difference between the degree variances d_n and c_n is negligible, which supports the contention that the local variations of gravity anomalies and gravity disturbances are quite similar.

Having made these comments, the remaining part of the report will be concerned only with errors in the contribution to N from the gravity field outside the spherical cap σ_c . Furthermore, only differences in undulations are treated, these being used in the definition of a relative geoid. This also effectively eliminates the need to consider errors in the zero-degree (constant) term of the undulation. Since N_2 (see equations (6) and (22)) is to be computed from a given set of potential harmonic coefficients, it is natural to estimate the errors in the frequency domain; that is, we start with N_2 as defined by equation (22).

Let P and Q be two points on the earth (sphere) at which N_2 is determined. The error incurred in the difference $\Delta N_2 = N_{2P} - N_{2Q}$ is

$$\Delta\epsilon = (N_{2P} - N_{2Q}) - (N_{2P} - N_{2Q})_{TRUE} \qquad (27)$$

or

$$\Delta\epsilon = \epsilon_P - \epsilon_Q \qquad (28)$$

where ϵ_P and ϵ_Q are the errors in N_{2P} and N_{2Q} . The error ϵ_P is composed of two (presumable uncorrelated) errors; namely, the error ϵ_{1P} due to erroneous potential coefficients (commission error) and the error ϵ_{2P} resulting from the lack of higher-degree coefficients (omission or truncation error):

$$\Delta\epsilon = \Delta\epsilon_1 + \Delta\epsilon_2 = (\epsilon_{1P} - \epsilon_{1Q}) + (\epsilon_{2P} - \epsilon_{2Q}) \qquad (29)$$

The error estimates that are studied in this report are global averages of the errors, the average being defined by the operator M:

$$M(\cdot) = \frac{1}{4\pi} \iint_{\sigma} (\cdot)\, d\sigma \tag{30}$$

This so-called "space average" (Moritz 1978) serves also to define the covariance functions, such as equations (24) and (25).

Consider first the error ϵ_{2P} induced by the unavailability of harmonic coefficients of degree greater than $\bar{n}$; from (22) it follows that

$$\epsilon_{2P} = -\frac{R}{2\gamma} \sum_{n=\bar{n}+1}^{\infty} \bar{Q}_n\, \delta g_n \tag{31}$$

This expression is quite analogous to the expansion of the gravity disturbance into spherical harmonics as in equation (14). Recalling the covariance function for δg, equations (25) and (26), it is immediately evident that the covariance function for ϵ_2 (that is, the global average of the products $\epsilon_{2P}\, \epsilon_{2Q}$ for points P, Q which are separated by a fixed spherical distance ψ_{PQ}) on the earth is given by

$$M(\epsilon_{2P}\, \epsilon_{2Q}) = \frac{R^2}{4\gamma^2} \sum_{n=\bar{n}+1}^{\infty} \bar{Q}_n^{\,2}\, d_n P_n(\cos \psi_{PQ}) \tag{32}$$

When P and Q coincide ($\psi_{PQ} = 0$), then $M(\epsilon_2^{\,2})$ is the variance of the error ϵ_2 (independent of the location of point P on the earth)

$$M(\epsilon_2^2) = \frac{R^2}{4\gamma^2} \sum_{n=\bar{n}+1}^{\infty} \bar{Q}_n^{\,2}\, d_n \tag{33}$$

On the other hand, the variance (global mean square) of the difference error $\Delta\epsilon_2$ is

$$M((\Delta\epsilon_2)^2) = M(\epsilon_{2P}^2) + M(\epsilon_{2Q}^2) - 2\, M(\epsilon_{2P}\, \epsilon_{2Q}) \tag{34}$$

which when equations (32), (33), and (26) are substituted becomes

$$M((\Delta\epsilon_2)^2) = \frac{R^2}{2\gamma^2} \sum_{n=\bar{n}+1}^{\infty} \bar{Q}_n^{\,2} \left(\frac{n+1}{n-1}\right)^2 c_n\, (1 - P_n(\cos \psi_{PQ})) \tag{35}$$

The degree variances c_n in this equation refer to the mean earth sphere of radius R. If, on the other hand, they are computed according to the model of Tscherning and Rapp (1974), for example, then the sphere of reference is the Bjerhammar sphere (the sphere entirely embedded within the earth). To rectify equation (35), the factors $\sigma^{n+2} = (R_B^2/R^2)^{n+2}$ are introduced (Jekeli 1978). Henceforth, unless otherwise stated c_n is understood to refer to the sphere of radius R_B; then

$$m_2^2 = M((\Delta\epsilon_2)^2) = \frac{R^2}{2\gamma^2}\sum_{n=\bar{n}+1}^{\infty} \bar{Q}_n^2 \left(\frac{n+1}{n-1}\right)^2 c_n \sigma^{n+2} (1 - P_n(\cos\psi_{PQ})) \qquad (36)$$

m_2 is the global estimate of the error in ΔN_2 due to a lack of higher-degree potential coefficients. This equation is obviously valid for any value of $R \geq R_B$, but we restrict ourselves to the earth's surface, where $R = 6371$ km.

For comparison, the corresponding error estimate derived by Christodoulidis (1976) is

$$(m_2')^2 = \frac{R^2}{2\gamma^2}\sum_{n=\bar{n}+1}^{\infty} Q_n^2 c_n \sigma^{n+2} (1 - P_n(\cos\psi_{PQ})) \qquad (37)$$

where the $Q_n(\psi_0)$, $n = 2,3,\ldots$ are Molodenskii's truncation coefficients.

The remaining error ϵ_1, caused by noise in the available potential coefficients can be estimated similarly. Let $\bar{C}_{nm}$, $\bar{S}_{nm}$ be the true, fully normalized harmonic coefficients (see also equ. (17)) and let $\bar{C}'_{nm}$, $\bar{S}'_{nm}$ be the corresponding coefficients that are available from combined, global gravity and satellite data (see also section 6). Then explicitly, using equation (19), the error in N_2 can be expanded in the series (note that the zero-degree term has been omitted)

$$\epsilon_1 = \frac{R}{2}\sum_{n=2}^{\infty}(n+1)\bar{Q}_n \sum_{m=0}^{n}[(\bar{C}'_{nm} - \bar{C}_{nm})\cos m\lambda + (\bar{S}'_{nm} - \bar{S}_{nm})\sin m\lambda]\bar{P}_{nm}(\cos\theta) \qquad (38)$$

If the covariance function on the earth of this error component is written in the form

$$M(\epsilon_{1P}\epsilon_{1Q}) = \sum_{n=2}^{\infty} \xi_n P_n(\cos\psi_{PQ}) \qquad (39)$$

where ψ_{PQ} is the spherical distance between points P and Q, then the degree variances ξ_n are given by (see e.g. Moritz 1972).

$$\xi_n = \frac{R^2}{4}(n+1)^2 \bar{Q}_n^2 \sum_{m=0}^{n}[(\bar{C}'_{nm} - \bar{C}_{nm})^2 + (\bar{S}'_{nm} - \bar{S}_{nm})^2], \quad n \geq 2 \qquad (40)$$

Suppose that $\bar{n}$ is the maximum degree to which these coefficients have been determined, then obviously we can take

$$\bar{C}'_{nm} = 0 = \bar{C}_{nm}, \quad \bar{S}'_{nm} = 0 = \bar{S}_{nm}, \quad \text{for } n > \bar{n} \qquad (41)$$

since the error due to neglected coefficients past degree $\bar{n}$ has already been accounted for.

The true values $\bar{C}_{nm}$ and $\bar{S}_{nm}$ are unknown, therefore, the differences appearing in equation (40) must be replaced by the corresponding estimated standard errors of the coefficients. It is shown later that under certain conditions,

we can assume equal standard errors for $\bar{C}'_{nm}$ and $\bar{S}'_{nm}$ for each degree n:

$$m_{\bar{C}_{nm}} = m_n = m_{\bar{S}_{nm}}, \quad 2 \le n \le \bar{n} \tag{42}$$

Then if $\hat{\xi}_n$ denotes the estimate of ξ_n based on (42),

$$\hat{\xi}_n = \frac{R^2}{4}(n+1)^2(2n+1)\, m_n^2\, \bar{Q}_n^2, \quad 2 \le n \le \bar{n} \tag{43}$$

and in view of (41), $\hat{\xi}_n = 0$ for $n > \bar{n}$; which yields finally the following estimate of the covariance function (39) on the earth:

$$\hat{M}(\epsilon_{1_P}\ \epsilon_{1_Q}) = \frac{R^2}{4}\sum_{n=2}^{\bar{n}}(n+1)^2(2n+1)m_n^2\bar{Q}_n^2\, P_n(\cos\psi_{PQ}) \tag{44}$$

As in the case of $\Delta\epsilon_2$ (see equation (34)), the estimated global mean square of the difference error $\Delta\epsilon_1$ is

$$\begin{aligned}\hat{M}[(\Delta\epsilon_1)^2] &= 2[\hat{M}(\epsilon_{2_P}^2) - \hat{M}(\epsilon_{2_P}\epsilon_{2_Q})] \\ &= \frac{R^2}{2}\sum_{n=2}^{\bar{n}}(n+1)^2(2n+1)\, m_n^2\, \bar{Q}_n^2\,(1 - P_n(\cos\psi_{PQ}))\end{aligned} \tag{45}$$

Again, if the potential coefficients refer to a sphere of radius R_B (in the sense that R in equation (17) is replaced by R_B), while the undulation differences are determined on a sphere of radius R, consistency is restored by multiplying $\hat{\xi}_n$ by σ^n (see Appendix B) where $\sigma = R_B^2/R^2$:

$$m_1^2 = \hat{M}[(\Delta\epsilon_1)^2] = \frac{R^2}{2}\sum_{n=2}^{\bar{n}}\bar{Q}_n^2(n+1)^2(2n+1)\, m_n^2\, \sigma^n(1 - P_n(\cos\psi_{PQ})) \tag{46}$$

m_1 is then a global estimate of the error in ΔN_2 that results from the random errors in the given potential harmonic coefficients. Christodoulidis (1976) derives the following estimate of the corresponding error in terms of the Molodenskii truncation coefficients Q_n, written here for comparison and later reference:

$$(m_1')^2 = \frac{R^2}{2}\sum_{n=2}^{\bar{n}}Q_n^2\,(n-1)^2(2n+1)\, m_n^2\sigma^n(1 - P_n(\cos\psi_{PQ})) \tag{47}$$

As briefly remarked earlier, the estimates m_1 (equation (46)) and m_2 (equation (36)) may be regarded as uncorrelated errors; and therefore, the total estimated error in ΔN_2 is

$$m = \sqrt{m_1^2 + m_2^2} \tag{48}$$

Some final notes with respect to the computation of these errors are appropriate. Both the commission error m_1 and the truncation error m_2 are subject to further approximation in the type of analysis (simulation study) to be conducted here. The degree variances c_n for gravity anomalies and

m_n^2 for the errors in potential coefficients are obtained through simple models. The (global) model for c_n is usually determined on the basis of "observed" degree variances of low degree (e.g. Tscherning and Rapp 1974). However, the sum in (36) requires degree variances for the high frequencies of the gravity field; this makes the choice of the model somewhat problematic in that it should actually reflect primarily these high-degree variations of gravity anomalies. The model for m_n^2, on the other hand, depends to some extent on the method by which the potential coefficients are determined. Christodoulidis (1976) constructed a model first tailored specifically to agree with the accuracies of the GEM 6 solution ((16,16) combined solution) and then generalized in a natural way for similar higher-degree solutions. We shall see later, in the light of newer and improved data, that this model may no longer be entirely appropriate. One further approximation in the evaluation of m_e^2 replaces the upper limit ∞ of the sum by a number, but with a fast computer there is no difficulty in making this number sufficiently large.

6. The Models for c_n and m_n^2

Little need be said in regard to the c_n-model - only that the model of Tscherning and Rapp (1974) was used here exclusively. The effects of a different model (the one proposed by Moritz (1976)) on the truncation error will be investigated briefly in section 9.

The model for m_n^2 that was selected by Christodoulidis (1976) has the form (F is a constant)

$$m_n^2 = \frac{(F/\bar{n})^4 n^4 c_n}{\gamma^2 (n-1)^2 (2n+1)} \quad , \quad 2 \le n \le \bar{n} , \quad \bar{n} \ge 16 \qquad (49)$$

Noting that the degree variances for gravity anomalies are given by

$$c_n = \gamma^2 (n-1)^2 \sum_{m=0}^{n} (\bar{C}_{nm}^2 + \bar{S}_{nm}^2) , \quad n \ge 2 \qquad (50)$$

it is readily seen that when $n = \bar{n}$ in (49), F^2 is the relative error of the potential coefficients of degree $\bar{n}$. Therefore, this model was designed on the basis that every solution for the potential coefficients yields approximately the same relative error at the maximum degree (Christodoulidis chose $F = .8$, implying a 64% relative error at $\bar{n}$).

Potential coefficients can naturally be determined from purely terrestrial gravity data, as well (Rapp 1969):

$$\begin{Bmatrix} \bar{C}_{nm} \\ \bar{S}_{nm} \end{Bmatrix} = \frac{1}{4\pi\gamma (n-1)} \iint_\sigma \Delta g \, \bar{P}_{nm} (\cos\theta) \begin{Bmatrix} \cos m\lambda \\ \sin m\lambda \end{Bmatrix} d\sigma \qquad (51)$$

Given a global distribution of mean gravity anomalies, the integral must be

approximated by some type of sum, e.g.

$$\begin{Bmatrix} \bar{C}_{nm} \\ \bar{S}_{nm} \end{Bmatrix} = \frac{1}{4\pi\gamma\,(n-1)} \sum_{\sigma} \overline{\Delta g}\, \bar{P}_{nm}(\cos\bar{\theta}) \begin{Bmatrix} \cos m\bar{\lambda} \\ \sin m\bar{\lambda} \end{Bmatrix} \Delta\sigma \qquad (52)$$

where $\overline{\Delta g}$ is the observed mean gravity anomaly for the block $\Delta\sigma$ that is centered at $(\bar{\theta},\bar{\lambda})$. The potential coefficients are computed through a least squares adjustment. It is not difficult to show (Rapp 1969) that the standard error (i.e. the square root of the diagonal element of the covariance matrix) of the coefficients of degree n is given by

$$m_n = \sqrt{\frac{\epsilon^2_{\Delta g}\,\Delta\theta\,\Delta\lambda}{4\pi\gamma^2(n-1)^2}}\ , \quad n \geq 2,\ \Delta\theta,\Delta\lambda \text{ in radians} \qquad (53)$$

This formula is derived with the assumption that the mean gravity anomalies are observed over the whole earth with the same accuracy $\epsilon_{\Delta g}$. Also, the error due to the fact that these observations constitute a noncontinous data set is ignored. It will be assumed that any such fault in the standard error above is incorporated into the overall uncertainty of the modeled error variance.

For a given solution of the coefficients $\bar{C}_{nm}$, $\bar{S}_{nm}$ all quantities (except n) on the right side of (53) are constant; thus, we may say that the error in the potential coefficients of degree $n \geq 2$, as determined from a global set of mean anomalies, is inversely proportional to $(n-1)$. Hence, the following simple model suggests itself for this case:

$$m_n = \frac{K}{n-1}\ , \quad K = \text{constant}, \quad 2 \leq n \leq \bar{n} \qquad (54)$$

Table 1 below compares the models given by equation (49) and (54) against the errors $\hat{m}_n$ of the solution obtained from GEM 9 plus $1^\circ \times 1^\circ$ mean anomalies (Rapp 1978, private communication) up to $n = 12$. In equation (49), we take $F = .8$, $\bar{n} = 20$ (GEM 9 is a (20,20) satellite solution),

Table 1. Comparison of Models (49) and (54) with $\hat{m}_n$ (obtained for the solution using GEM 9 plus $1^\circ \times 1^\circ$ mean anomalies)

n	$\hat{m}_n \times 10^6$	$m_n \times 10^6$, model (49)	$m_n \times 10^6$, model (54)
2	.0027	.0080	.0581
3	.0066	.0155	.0291
4	.0046	.0138	.0194
5	.0072	.0136	.0145
6	.0057	.0137	.0116
7	.0067	.0139	.0097
8	.0057	.0142	.0083
9	.0057	.0145	.0073
10	.0051	.0148	.0065
11	.0050	.0151	.0058
12	.0044	.0154	.0053

and the c_n-model of Tscherning and Rapp (1974) (see equation (59)). In equation (54), $K = .0581 \times 10^{-3}$. This value of K is the average of the values of K implied by the standard errors from $n = 13$ to $n = 60$ of potential coefficients computed from $1^\circ \times 1^\circ$ gravity data alone (Rapp 1978, private communication). Table 2 shows the relevant information by comparing the resulting model (54) with the standard errors of the potential coefficients.

Table 2. Comparison of model (54) ($K = .0581 \times 10^{-6}$) with $\hat{m}_n$ obtained for the solution using $1^\circ \times 1^\circ$ mean anomalies (Rapp 1978).

n	$\hat{m}_n \times 10^6$	$m_n \times 10^6$, model (54)	n	$\hat{m}_n \times 10^6$	$m_n \times 10^6$, model (54)
13	.00483	.00484	37	.00162	.00161
14	.00446	.00447	38	.00157	.00157
15	.00414	.00415	39	.00153	.00153
16	.00386	.00387	40	.00149	.00149
17	.00362	.00363	41	.00145	.00145
18	.00341	.00342	42	.00142	.00142
19	.00322	.00323	43	.00138	.00138
20	.00305	.00306	44	.00135	.00135
21	.00290	.00290	45	.00132	.00132
22	.00276	.00277	46	.00129	.00129
23	.00264	.00264	47	.00126	.00126
24	.00252	.00253	48	.00124	.00124
25	.00242	.00242	49	.00121	.00121
26	.00232	.00232	50	.00119	.00119
27	.00223	.00223	51	.00116	.00116
28	.00215	.00215	52	.00114	.00114
29	.00207	.00207	53	.00112	.00112
30	.00200	.00200	54	.00110	.00110
31	.00193	.00194	55	.00108	.00108
32	.00187	.00187	56	.00106	.00106
33	.00181	.00182	57	.00104	.00104
34	.00176	.00176	58	.00102	.00102
35	.00171	.00171	59	.00101	.00100
36	.00166	.00166	60	.00099	.00098

The GEM 9 solution combined with the $1^\circ \times 1^\circ$ terrestrial data yields one of the most recent and realistic accuracy estimates for the potential coefficients. This solution supplies coefficients up to a maximum degree $\bar{n} = 60$; but solutions up to $\bar{n} = 180$ have been done (Rapp 1979, private communication). An inspection of Table 1 reveals the inadequacy of model (49). Different values for the model parameters F and $\bar{n}$ could conceivably diminish the discrepancies, but such changes in the parameters are not easily justified from a theoretical standpoint since the model is purely an empirical construction. Consequently, the model (49) is not studied further in this report. Table 2 exhibits the excellent agreement between the model (54) and the errors of potential coefficients

(for $13 \le n \le 60$) that are derived from terrestrial data. However, model (54) compares not as well with the low-degree ($n \le 6$) errors obtained through the combined solution (see Table 1) which are favorably influenced by the "a priori" coefficient errors from the satellite solution. In specialized investigations, it is not unfeasible to use a model such as (54) for the high-degree errors and the actual standard deviation, $\hat{m}_n$, as given in Table 1 (first column) for the errors at the low-degree end of the spectrum:

$$m_n = \begin{cases} \hat{m}_n, & 2 \le n \le n_1 \\ \dfrac{K}{n-1}, & n_1 < n \le \bar{n} \end{cases} \qquad (55)$$

7. Computational Analyses of the Errors

The radical dissimilarity between model (54) and model (49) which was used by Christodoulidis (1976) warrants some new tests here with his error equations (37) and (47). (It should be remarked that these equations are completely valid provided that gravity anomaly data referred to the geoid are available within the cap σ_c.) Since m_1 and m_2 are the square roots of squared errors averaged over the earth, they are designated root mean square (RMS) errors in the figures. They are also called simply error estimates in the following discussion. To avoid unnecessarily cumbersome language, the following designations are introduced:

$$\begin{aligned} &\text{Method A} = \text{the method of computing error estimates of } \Delta N \text{ based on gravity anomaly data within the cap } \sigma_c \text{ (equations (37) and (47))} \\ &\text{Method B} = \text{the method of computing error estimates of } \Delta N \text{ based on gravity disturbance data within the cap } \sigma_c \text{ (equations (36) and (46))} \end{aligned} \qquad (56)$$

The error estimates of ΔN_2 may be investigated with respect to variations in the separation ψ_{PQ}, in the cap radius ψ_0, in the maximum degree $\bar{n}$ of the potential coefficients, and in the model (54) itself.

Method A was used to determine the general characteristics of the ΔN_2 - errors as they are implied by the model (55) with $K = .0581 \times 10^{-6}$, $n_1 = 12$, and $\hat{m}_n$ given in Table 1. Figure 2 depicts, for $\psi_0 = 30^\circ$, the commission and truncation errors in ΔN_2 as functions of the separation ψ_{PQ} and the maximum degree $\bar{n}$. For these and all subsequent evaluations of the truncation error, the upper limit ∞ in (36) and (37) is "approximated" by 3000 at which point a precision of at least .1 mm seems to be attained. Evidently, since the truncation error is independent of the standard errors of the available potential coefficients, the corresponding curves trace the same values given by Christodoulidis (1976, Table 7, $\bar{n} = 30$). The commission errors, however, increase with increasing $\bar{n}$, as opposed to the corresponding decrease in the commission

Figure 2. Commission (Solid line) and Truncation (Dotted line) Undulation Difference Errors Using Current Potential Coefficient Error Estimates and Assuming Perfect Gravity Anomaly Data Within a 30° Cap.

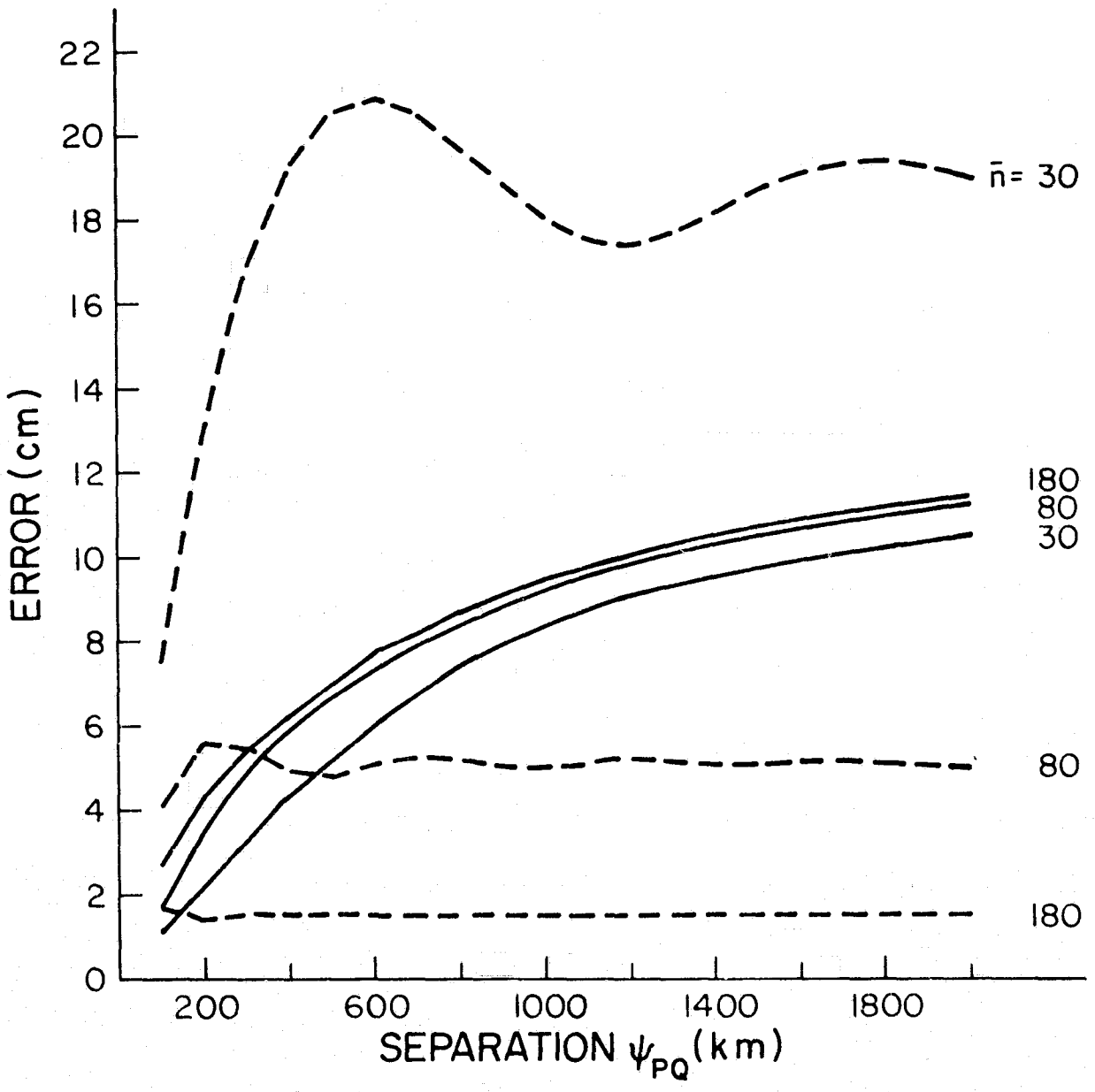

errors of Christodoulidis (see his Table 6). These contrasting characteristics are obviously the direct consequence of the difference in the error models, specifically, because the model (54) or (55) does not stipulate the same relative accuracy at all values of $\bar{n}$. As seen in Figure 2, the commission errors do appear to be bounded (as $\bar{n}$ varies), at least for larger values of ψ_{PQ}. It is observed that the truncation error loses its dependence on the separation ψ_{PQ} as the number of available potential coefficients increases. Contrarily, the commission error varies significantly (but not without bound), regardless of the value of $\bar{n}$, as the spherical distance between points P and Q increases.

The root sum of squared truncation and commission errors of Figure 2 is presented in Figure 3 for both Methods A and B. Figures 4 and 5 are analogous to Figures 2 and 3 in that the same error model (55) is used in the computation of the errors. But here, the errors are shown as functions of the separation ψ_{PQ} and of the cap radius ψ_0, $\bar{n}$ being fixed at 180. A "cap radius" of $\psi_0 = 0$ signifies that there is no cap and implies that the undulations are determined from potential coefficients only. Again, the truncation errors are practically independent of the separation ψ_{PQ} (since $\bar{n} = 180$, cf. Fig. 2). The commission errors exhibit a similar type of dependence on ψ_{PQ} as in Figure 2; and they must plainly increase strongly as the size of the cap σ_c decreases implying less and less detailed gravity data near the computation points. The total (RMS) error as a function of ψ_{PQ} and ψ_0, shown in Figure 5, in this case resembles the dominating commission error.

It is noted that for $\psi_0 = 0$ (no cap), the errors according to Method B are equal to those of Method A since no terrestrial gravity measurements "within the cap" enter into the computations of the undulations. In fact, the error equations (36), (46) are identical to (37), (47) when $\bar{Q}_n(0) = 2/(n+1)$ and $Q_n(0) = 2/(n-1)$ are substituted (see also Figure 7).

Having established the general characteristics of the commission and truncation errors in Figures 2 and 4, the remaining investigations concentrate on the total (RMS) errors in ΔN_2 with $\bar{n}$ fixed at 180. In addition, the potential coefficient error model (54) is now used for the entire spectrum, $n = 2, \ldots, 180$. More explicitly, this model can be written (with $\gamma = 979800$ mgal, $\Delta\theta = \Delta\lambda = 1^\circ = .01745$ rad. in equation (53)) as

$$m_n = \frac{0.00502 \times 10^{-6}}{n-1} \epsilon_{\Delta g} \qquad (57)$$

where $\epsilon_{\Delta g}$ as a new variable in the analysis is the average error in the mean $1^\circ \times 1^\circ$ gravity anomalies. Figure 6 displays two sets of errors computed by Method A, for $\psi_0 = 0^\circ$ and $\psi_0 = 30^\circ$. The curve for $\psi_0 = 0^\circ$, $\epsilon_{\Delta g} = 1$ mgal essentially traces the truncation error which in this case almost completely overshadows the commission error; and therefore, it represents the maximum attainable accuracy in undulation differences which are derived solely from potential coefficients up to degree 180. Recall that the standard errors as modeled by (54) for small degree are much larger than what might be expected

Figure 3. Total RMS Errors for Geoid Undulation Differences Assuming Perfect Gravity Data Within a 30° Cap Using Gravity Anomalies (Method A) and Gravity Disturbances, (Method B), and Current Potential Coefficient Error Estimates.

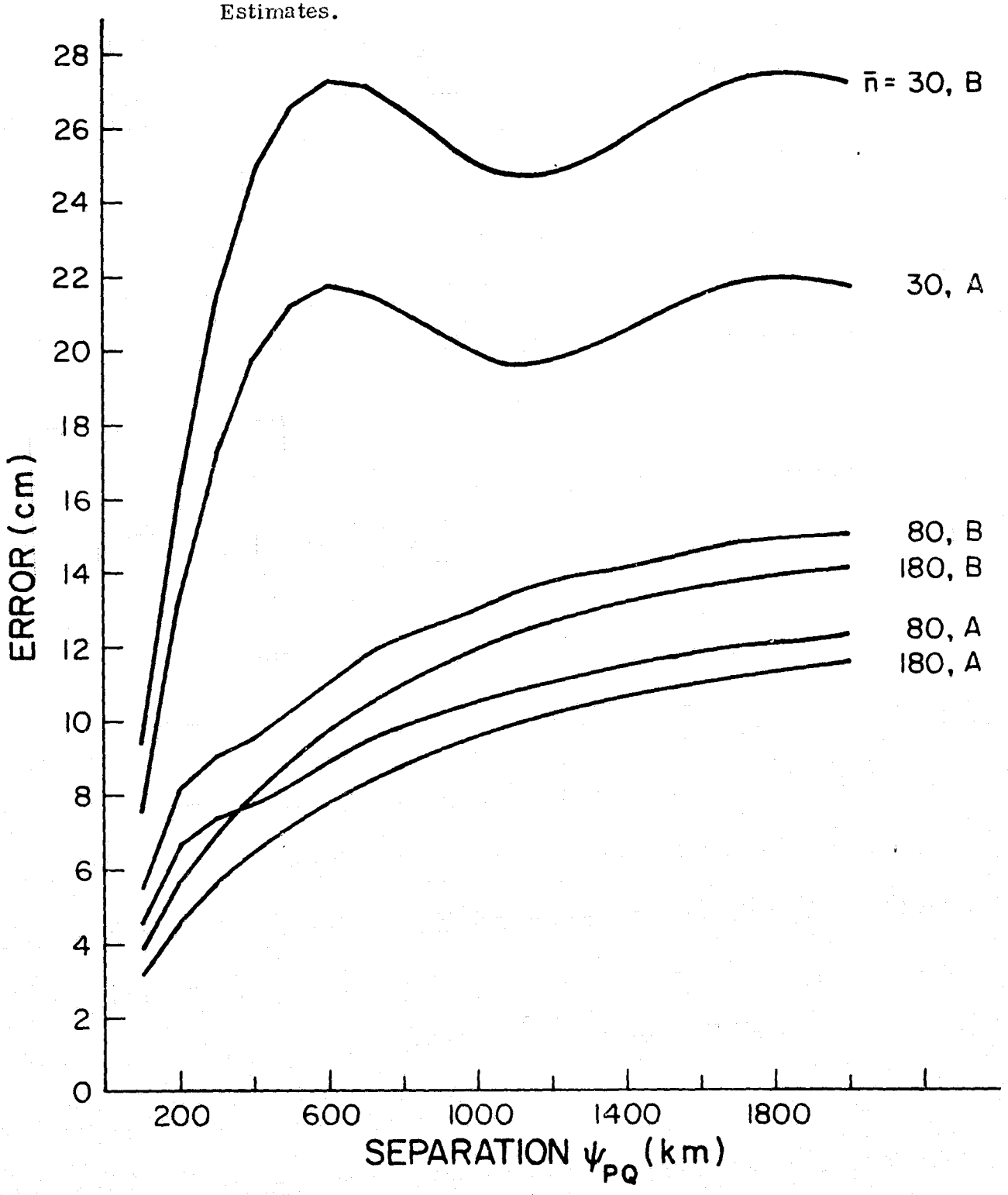

Figure 4. Commission (Solid line) and Truncation (Dotted line) Undulation Difference Errors Assuming Perfect Gravity Anomaly Data Within a Cap of Radius ψ_0 and Potential Coefficients Estimated to Degree 180.

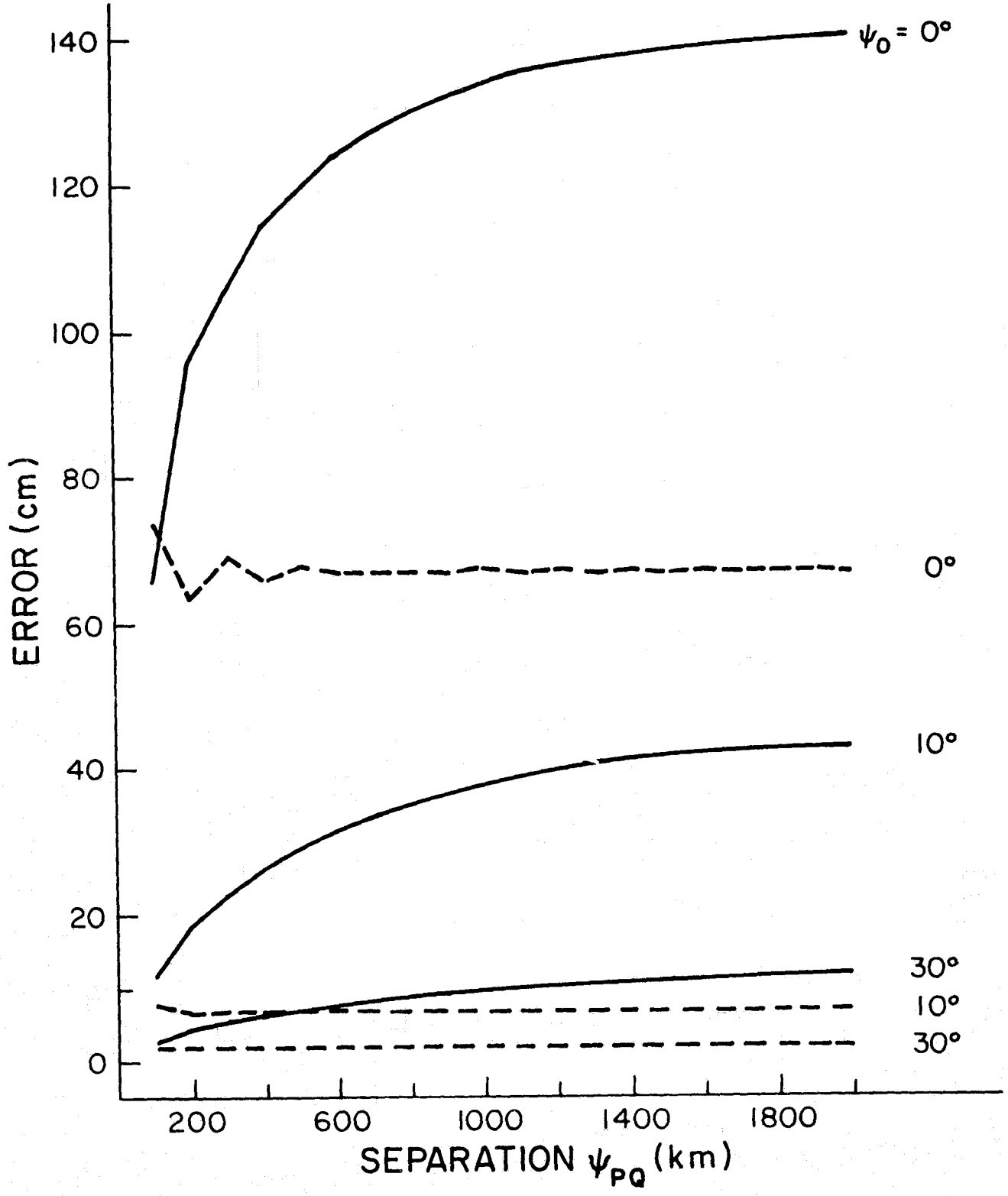

Figure 5.

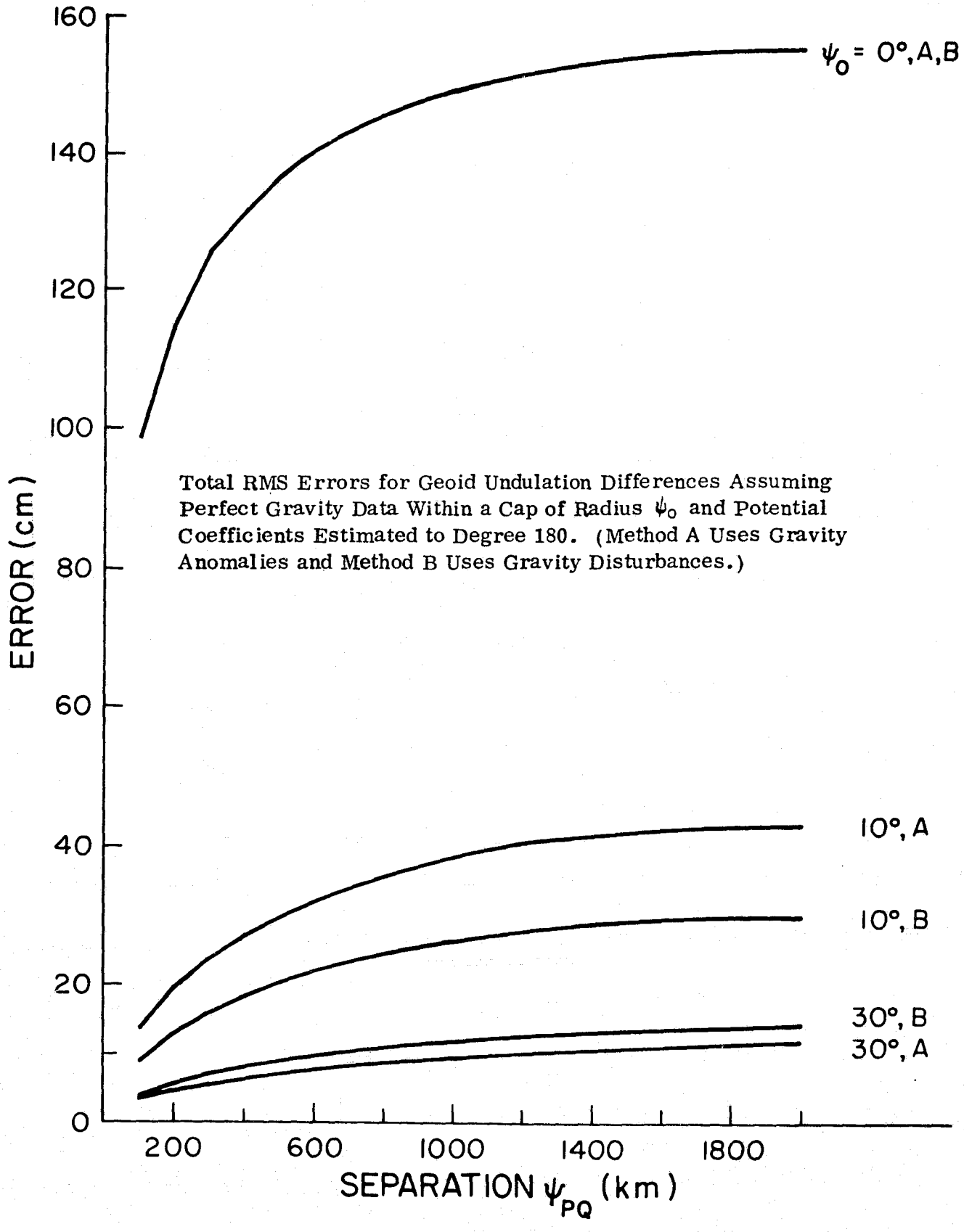

Total RMS Errors for Geoid Undulation Differences Assuming Perfect Gravity Data Within a Cap of Radius ψ_0 and Potential Coefficients Estimated to Degree 180. (Method A Uses Gravity Anomalies and Method B Uses Gravity Disturbances.)

Figure 6.

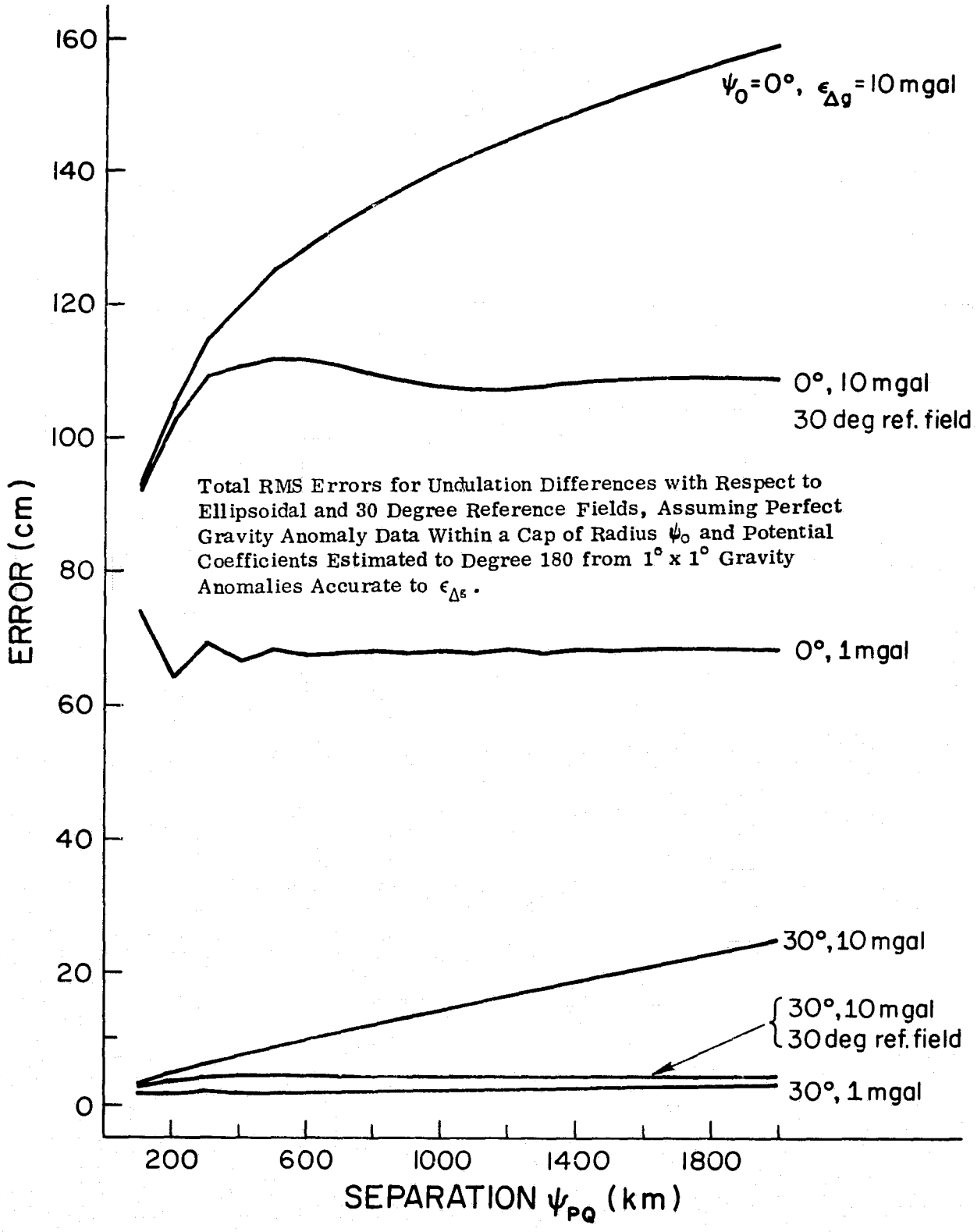
160
140
120
100
80
60
40
20
0
ERROR (cm)
ψ_0=0°, $\epsilon_{\Delta g}$=10 mgal
0°, 10 mgal
30 deg ref. field
Total RMS Errors for Undulation Differences with Respect to Ellipsoidal and 30 Degree Reference Fields, Assuming Perfect Gravity Anomaly Data Within a Cap of Radius ψ_0 and Potential Coefficients Estimated to Degree 180 from 1° x 1° Gravity Anomalies Accurate to $\epsilon_{\Delta g}$.
0°, 1 mgal
30°, 10 mgal
30°, 10 mgal
30 deg ref. field
30°, 1 mgal
200
600
1000
1400
1800
SEPARATION ψ_{PQ} (km)

from a combined solution (see Table 1, columns 1 and 3). We find that this is the reason for the steeper increase of the ($\psi_0 = 0$, $\epsilon_{\Delta g} = 10$ mgal) - curve at the larger values of ψ_{PQ} when compared to the corresponding curve of Figure 5 (where $K = .0581 \times 10^{-6}$ implies $\epsilon_{\Delta g} = 11.6$ mgal). Finally, Figure 6 includes curves for errors in ΔN_2 when the undulations are referred to a perfect 30-degree potential reference field. These errors are computed by replacing the lower limit of the sum in equation (37) by $n = 31$. Results (not shown) similar to those of Figure 6 can easily be produced also for Method B; the same general characteristics should be expected.

Figures 3 and 5 have shown that the errors, whether through Method A or through Method B, possess a parallel dependence on both the maximum degree $\bar{n}$ and the separation ψ_{PQ}; Figure 7 finally compares Methods A and B in regard to the dependence on the cap radius ψ_0. These curves represent the errors only for a particular separation, $\psi_{PQ} = 1500$ km. Other values of ψ_{PQ} would not alter the basic interrelationships shown here.

As observed in Figure 3, the total errors of Method B are greater than the corresponding total errors of Method A when the cap radius is 30° and the model (55) is chosen. However, Figure 7 (where the model (54) is used) and Figure 5 both show that this is not normally the case.

It should be strongly emphasized that, except for the case $\psi_0 = 0$, all figures depict estimated, average errors associated with only the outer zone contribution, ΔN_2, to the total undulation difference. Recall that ψ_0 equal to zero implies that $\Delta N_2 = \Delta N$ is the total undulation difference. Up to this point, no numerical description has been given to the errors that are encountered within the spherical cap.

If the data of this inner zone were continuous and errorless, thus yielding exact values of ΔN_1, the error in ΔN_2, of course, would also be the error in the total undulation difference. In the absence of this ideal situation, two types of errors in the gravity data enter into the computation of N_1; namely, the discretion error resulting from the lack of continuous data, and a propagated error due to imperfect measurements. The latter includes the influence of errors in altimeter measurements (see section 2).

It is important to realize that the principle of truncation functions as utilized here, and in general, is based on the assumption that the gravity material in the vicinity of the computation point (i.e. within the spherical cap) is more dense and accurate than in the remote zones. Indeed, for a global, uniformly accurate field of mean anomalies it is pointless, if not invalid, to compute first potential coefficients (and subsequently N_2) from this global set and then N_1 from the same mean gravity anomalies in a spherical cap. In this special case of uniform coverage with no possibility of local densification, we must choose $\psi_0 = 0$.

Figure 7. Total RMS Errors for Geoid Undulation Differences at 1500 km Assuming Perfect Gravity Data Within a Cap of Radius ψ_0 with Potential Coefficients Estimated to Degree 180 Based on Anomalies Given to an Accuracy of $\epsilon_{\Delta g}$.

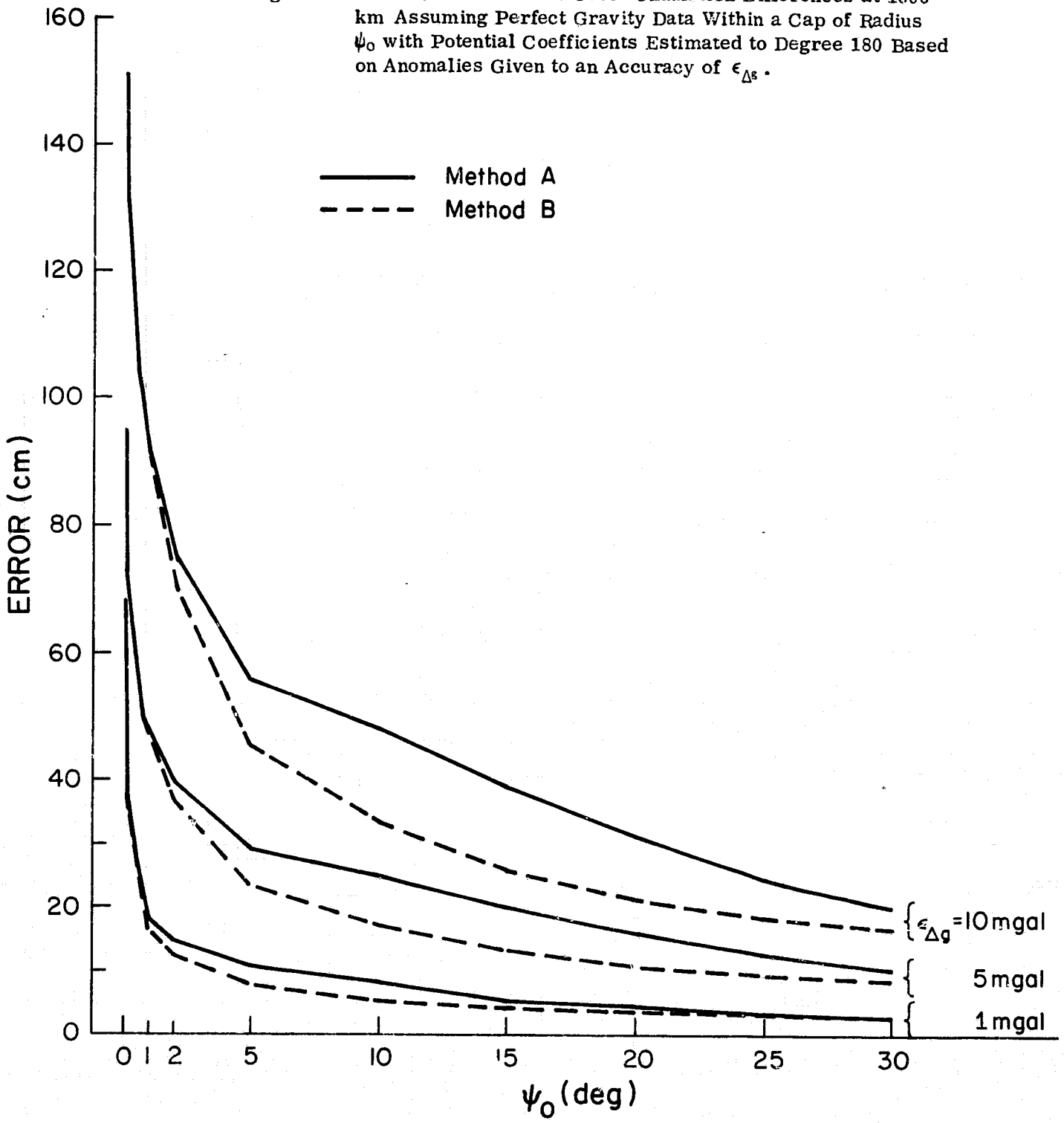

Rapp (1973) and Christodoulidis (1976) have examined these errors with respect to the inner zone. Christodoulidis formulates the errors in the differences ΔN_1 based on Method A. The argument of section 5, that the errors of ΔN_1 do not differ substantially in going from Method A to Method B, can be used to obtain average estimates of the discretion and propagated errors of ΔN_1 by quoting results from Christodoulidis (1976). Only an example is given here to illustrate the orders of magnitude that may be expected.

Assume that potential coefficients are available to degree 180 as obtained from a global field of $1^\circ \times 1^\circ$ mean anomalies that have a uniform accuracy of ± 5 mgal. Further, suppose that two spherical caps, each having a radius of $\psi_0 = 25^\circ$ are covered by $30' \times 30'$ mean gravity disturbances with an average accuracy of ± 1 mgal. Let's say that the cap centers are separated by 1500 km. The discretion and propagated errors associated with ΔN_1 (see Tables 3 and 4 of Christodoulidis, 1976) are 32.2 cm and 27.4 cm, respectively. From Figure 7, the total error in ΔN_2 is 9.2 cm. Provided that ΔN_1 and ΔN_2 are uncorrelated, the average, estimated error in ΔN, the total undulation difference, is 43.3 cm.

8. Mean Undulation Difference Errors

Thus far, the error analysis has been confined to differences between point undulations. The mean undulation function which represents an average of undulations over a spherical cap is characteristically derived from the point undulation function by introducing a smoothing factor β_n into its spherical harmonic expansion. Details of this procedure may be found in Meissl (1971). Very briefly, the average undulation over a cap σ_1 of radius ψ_1 on the sphere can be expressed as

$$\bar{N}(\bar{\theta},\bar{\lambda}) = \frac{1}{2\pi(1-\cos\psi_1)} \iint_{\sigma_1} N(\theta,\lambda)\, d\sigma \qquad (58)$$

where $2\pi(1-\cos\psi_1)$ is the area of the cap σ_1 (on the unit sphere), and $(\bar{\theta},\bar{\lambda})$ are spherical coordinates associated with this cap, for example, its center coordinates. The eigenfunctions of the integral operator above (operating on N) are the spherical harmonics $\sin m\lambda\, \bar{P}_{nm}(\cos\theta)$ and $\cos m\lambda\, \bar{P}_{nm}(\cos\theta)$; while the corresponding eigenvalues are (for all orders $0 \le m \le n$, and $n > 0$)

$$\beta_n = \frac{1}{2n+1} \frac{1}{1-\cos\psi_1} [P_{n-1}(\cos\psi_1) - P_{n+1}(\cos\psi_1)] \qquad (59)$$

Therefore, when the spherical harmonic expansion of N (equation (17) with $N = T/\gamma$) is substituted into (58), the mean undulation becomes (zero- and first-degree terms are omitted, see section 5)

$$\bar{N}(\bar{\theta},\bar{\lambda}) = R \sum_{n=2}^{\infty} \beta_n \sum_{m=0}^{n} (\bar{C}_{nm}\cos m\bar{\lambda} + \bar{S}_{nm}\sin m\bar{\lambda})\, \bar{P}_{nm}(\cos\bar{\theta}) \qquad (60)$$

The only difference between N and $\bar{N}$ is in the harmonic coefficients. This fact implies that we may write (cf. equation (22)):

$$\left.\begin{aligned} \bar{N} &= \bar{N}_1 + \bar{N}_2 \\ \text{where} \qquad \bar{N}_1 &= \frac{R}{\gamma}\sum_{n=2}^{\infty}\left(\frac{1}{n+1} - \frac{1}{2}\bar{Q}_n\right)\beta_n\,\delta g_n \\ \bar{N}_2 &= \frac{R}{2\gamma}\sum_{n=2}^{\infty}\bar{Q}_n\,\beta_n\,\delta g_n \end{aligned}\right\} \quad (61)$$

This analogy can be extended to the point that the average, estimated errors in $\Delta\bar{N}_2$ $(=\bar{N}_{2P} - \bar{N}_{2Q})$ due to erroneous potential coefficients up to degree $\bar{n}$ and due to a lack of higher-degree coefficients are given by (cf. equations (46) and (36), respectively)

$$\left.\begin{aligned} \bar{m}_1^2 &= \frac{R^2}{2}\sum_{n=2}^{\bar{n}}\bar{Q}_n^2\,(n+1)^2(2n+1)\beta_n^2 m_n^2\,\sigma^n\,(1-P_n(\cos\psi_{PQ})) \\ \bar{m}_2^2 &= \frac{R^2}{2\gamma^2}\sum_{n=\bar{n}+1}^{\infty}\bar{Q}_n^2\left(\frac{n+1}{n-1}\right)^2\beta_n^2\,c_n\sigma^{n+2}\,(1-P_n(\cos\psi_{PQ})) \\ \gamma &= \frac{kM}{R^2} \end{aligned}\right\} \quad (62)$$

It is assumed that if $\psi_0 > 0$, then $\psi_1 < \psi_0$; that is, the mean undulation cap is smaller than the cap representing the inner zone. If $\psi_0 = 0$, then the mean undulation is computed solely from a finite set of potential coefficients. Similar error equations for $\Delta\bar{N}_2$ can be derived on the supposition that the inner zone is covered with gravity anomaly data (cf. equations (47) and (37), respectively):

$$(\bar{m}_1')^2 = \frac{R^2}{2}\sum_{n=2}^{\bar{n}}Q_n^2\,(n-1)^2(2n+1)\,\beta_n^2 m_n^2\sigma^n\,(1-P_n(\cos\psi_{PQ})) \quad (63)$$

$$(\bar{m}_2')^2 = \frac{R^2}{2\gamma^2}\sum_{n=\bar{n}+1}^{\infty}Q_n^2\,\beta_n^2\,c_n\,\sigma^{n+2}\,(1-P_n(\cos\psi_{PQ})), \quad \gamma = \frac{kM}{R^2} \quad (64)$$

Normally, the cap associated with the mean undulation is approximated by a block which has the same area. Therefore, for a $\theta_1^\circ \times \theta_1^\circ$ mean undulation, the corresponding cap radius ψ_1 is roughly (since $\theta_1^2 \approx \pi\psi_1^2$)

$$\psi_1 = \theta_1/\sqrt{\pi} \quad (65)$$

where θ_1 and ψ_1 have the same units. For $\theta_1 = 1^\circ$, $\psi_1 = 0^\circ.564$; and for $\theta_1 = 5^\circ$, $\psi_1 = 2^\circ.821$.

Mean undulations are presently envisaged to be derived from gravity anomaly data; and therefore, the estimated errors are displayed for Method A only. Moreover, of the many combinations of the variables ψ_0, $\bar{n}$, $\epsilon_{\Delta g}$, θ_1 that could be investigated, only a few of particular interest are shown in the figures.

For small values of θ_1, such as 1° or 2°, the attenuation of the smoothing factor β_n (equation (59)) is rather slow for the low frequencies (e.g. $\theta_1 = 1°$; $\beta_{10} = .999$, $\beta_{100} = .883$, $\beta_{300} = .240$). Therefore, the effect of β_n in the truncation error (equation (64)) is much more pronounced than in the commission error (equation (63)). This is verified in Figure 8, where two pairs of curves (for $\epsilon_{\Delta g} = 1$ mgal and $\epsilon_{\Delta g} = 10$ mgal) trace the estimated errors in the $\Delta\bar{N}_2$ contribution to 1° x 1° mean undulation differences. Figure 8 should be compared to Figure 6 which depicts error curves for point undulation differences. If $\epsilon_{\Delta g} = 10$ mgal (and $\bar{n} = 180$), the commission error dominates the truncation error and the total error generally falls by only 10% to 15% in going from point to 1° x 1° mean undulations. Note however, the more substantial decrease when the centers of the 1° x 1° blocks are close together (30% for $\psi_{PQ} = 100$ km). Similar results for $\theta_1 = 5°$, $\epsilon_{\Delta g} = 10$ mgal (not shown) mostly show an additional decline in the errors of about 20% to 30% (somewhat more for small ψ_{PQ}).

The more dramatic effect is in mean undulation errors which reflect predominantly the neglect of high-frequency gravity information. Evidence to this is given by the two curves of Figures 6 and 8 which correspond to the case $\psi_0 = 0$, $\epsilon_{\Delta g} = 1$ mgal and show a difference of 50% between them. A further reduction by 50% to estimated errors of 10 cm to 15 cm is obtained for 2° x 2° mean undulation differences. The curves in Figure 8 represent estimated errors in the total mean undulation difference $\overline{\Delta N}$ for the case $\psi_0 = 0$, but also when $\psi_0 = 20°$ if errorless differences $\overline{\Delta N}_1$ can be derived from the data of the inner zone.

Figure 9 exhibits a comparison of mean undulation difference errors ($\psi_0 = 0°$) with respect to various potential fields of reference. Little seems to be gained in accuracy when changing from a 20-degree to a 30-degree reference field. Again, because the truncation error overshadows the commission error when $\epsilon_{\Delta g} = 1$ mgal, the choice of the reference field, practically speaking, is immaterial in this case.

9. The Effect of a Different c_n-Model

As mentioned previously, the estimated truncation error relies on the choice of the model for the anomaly degree variances. To examine this dependence, the errors with the model of Moritz (1976),

$$c_n = \alpha_1 \frac{n-1}{n+A} \sigma_1^{n+2} + \alpha_2 \frac{n-1}{(n-2)(n+B)} \sigma_2^{n+2}, \quad n \geq 3 \qquad (66)$$

are compared to the errors with the model of Tscherning and Rapp (1974) which, so far, has been used without exception:

$$c_n = \alpha_2 \frac{n-1}{(n-2)(n+B)}, \quad n \geq 3 \qquad (67)$$

where $\alpha_2 = 425.28$ mgal^2, $B = 24$

Figure 8. Total RMS Errors for $1^\circ \times 1^\circ$ Mean Undulation Differences, Assuming Perfect Gravity Anomaly Data Within a Cap of Radius ψ_0 and Potential Coefficients to Degree 180 Estimated from $1^\circ \times 1^\circ$ Gravity Anomalies Accurate to $\epsilon_{\Delta g}$.

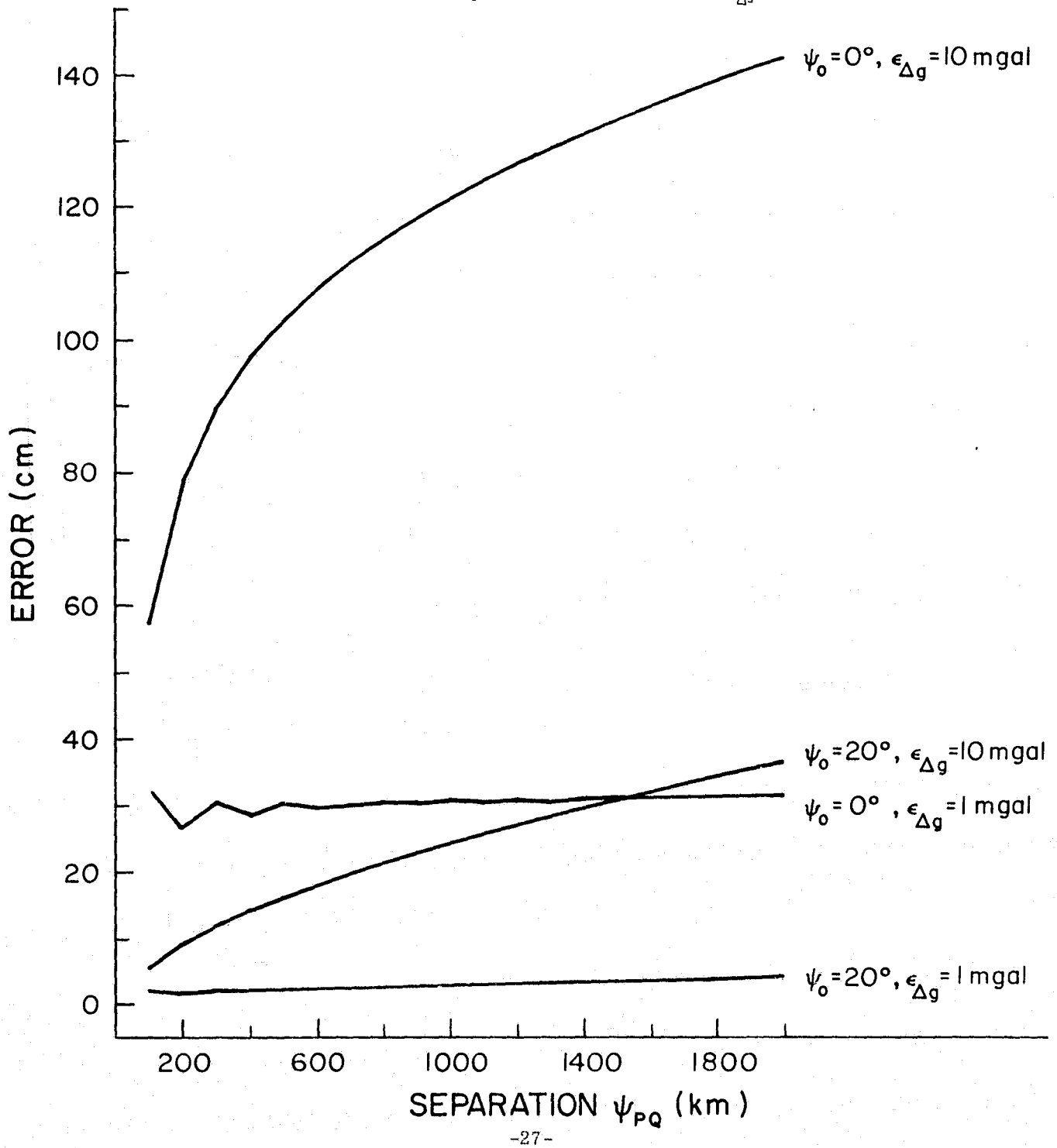

Figure 9. Total RMS Errors of 1° x 1° Mean Undulation Differences With Respect to Ellipsoidal, 20 Degree, and 30 Degree Reference Fields, Assuming a Set of Potential Coefficients to Degree 180 Estimated from 1° x 1° Gravity Anomalies Accurate to $\epsilon_{\Delta g}$.

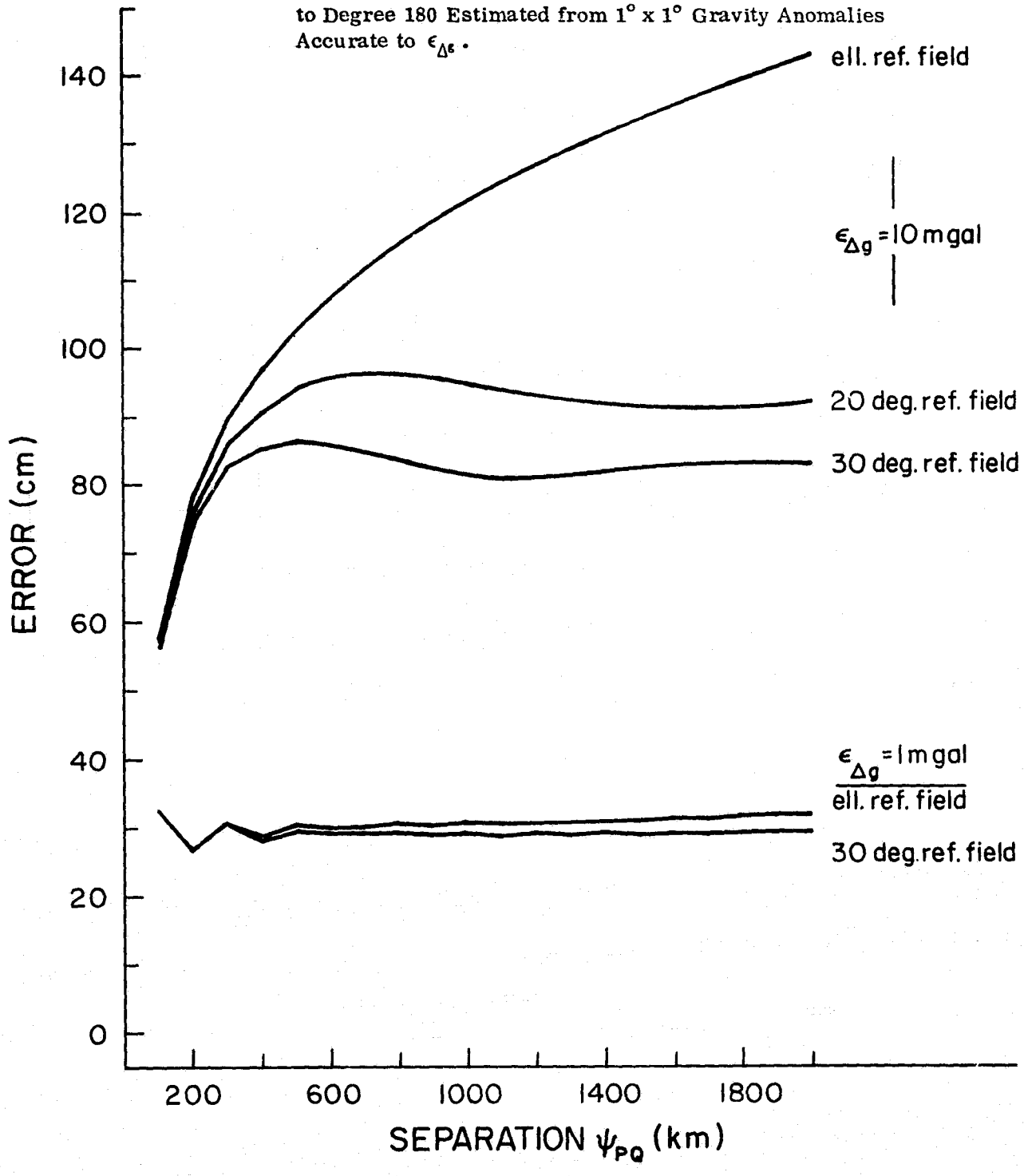

The parameters for the model (66), as given by Jekeli (1978), are

$$\alpha_1 = 18.3906 \text{ mgal}^2, \quad \sigma_1 = .9943667 \qquad A = 100$$
$$\alpha_2 = 658.6132 \text{ mgal}^2, \quad \sigma_2 = .9048949 \qquad B = 20$$

This model refers to the sphere of radius R (cf. p. 9). Comparing the two models, in general, it is clear that for large n , the first term of model (66) provides the dominant contribution; and therefore, the decrease of c_n in (66) is less rapid (for $100 < n < 600$) than in (67). The implication is that the truncation error, which is essentially the sum of the high-degree error variances, is greater when model (66) is used instead of model (67). This conclusion is verified by the values of Table 3 which are computed via equation (37) (Method A) with $\bar{n} = 180$ and $\psi_0 = 0°$. Similar results would evidently be obtained if other cap radii and equation (36) (Method B) were used.

Table 3. Truncation Errors of Undulation Differences ($\psi_0 = 0°$, $\bar{n} = 180$, Method A) based on two different c_n-Models.

ψ_{PQ} (km)	m_2' (cm) model (67)	m_2' (cm) model (66)
200	63.6	88.3
600	66.6	93.2
1000	67.1	94.0
1400	67.1	93.9
1800	69.9	93.6

It cannot be stated categorically that one of the above models is superior to the other since the characteristics of the gravity field on which they differ are not yet established with sufficient confidence. Therefore, the considerable differences between the last two columns in Table 3 suggest still some uncertainty in the estimation of the truncation errors.

10. Other Methods

By no means is the method based on Molodenskii's truncation theory the only approach to undulations from gravity disturbances. Collocation (Moritz 1972) is a method as amenable in this case as when gravity anomalies constitute the gravity data. Although this method is not discussed further (Christodoulidis (1976) shows that the corresponding error analysis is quite difficult for large amounts of data), the cross-covariance function between gravity disturbances and geoid undulations is given here for the sake of completeness (cf. equation (25)):

$$\text{cov}\,(N_P, \delta g_Q) = \frac{R^2}{\gamma_P r_Q} \sum_{n=2}^{\infty} \frac{n+1}{(n-1)^2} c_n \left(\frac{R^2}{r_P r_Q}\right)^{n+1} P_n(\cos\psi_{PQ}) \qquad (68)$$

The sum starts with $n = 2$ under the assumption that the zero- and first-degree potential harmonics are absent; also c_n refers to a sphere of radius R.

An error analysis was conducted by Sjöberg (1979), in which the geoid undulation is assumed to be computed from global mean gravity data. The lack of more detailed data than mean anomalies constitutes a type of truncation error; while erroneous data implies a commission error. The global mean of these errors in this case can be written in terms of the smoothing factors β_n. The commission error also relies on an error model similar to equation (53). Both error estimates are infinite series and are also developed for undulation differences by Sjöberg (1979). On the basis of a $1^\circ \times 1^\circ$ mean anomaly field with an accuracy of 1 mgal, computations using these formulas give a total error in ΔN of 55 cm ($\psi_{PQ} = 2000$ km). Assuming that the lack of detail beyond $1^\circ \times 1^\circ$ mean anomalies is equivalent to a truncation error with $\bar{n} = 180$, the curve for $\psi_0 = 0$, $\epsilon_{\Delta g} = 1$ mgal in Figure 6 shows an error in ΔN of 68 cm ($\psi_{PQ} = 2000$ km). The difference in these results ($\sim 20\%$) is not excessive in view of the totally dissimilar methods of analysis.

It was noted earlier (section 3) that the Molodenskii truncation theory provides for the series of a part of Stokes' integral to converge faster than the series expansion of the entire integral. Molodenskii, et al. (1962) discuss a further improvement in this convergence. A very elegant type of generalization of their principle was investigated by Colombo (1977). The concept of this method rests on the simple fact that a change in the Stokes' function (the kernel of the integral) naturally induces a change in the errors as embodied in part by the (now also changed) Q_n coefficients. Colombo parameterized the kernel and achieved, to some extent, the "best" Stokes' function by minimizing the errors in a least squares sense. These promising techniques can obviously be applied to the integral of gravity disturbances without any difficulty.

11. Summary and Conclusions

It was the intent of this report to subject the geoid undulation differences as they are determined by a surface integral of gravity disturbances to an error analysis in the frequency domain. The principles of the Molodenskii truncation theory are applied to the extent that the undulation N is decomposed into an integral over a spherical cap centered at the computation point and an infinite series of spherical harmonics which essentially represent the contribution to N from the gravity field outside this cap. A study of the data requirements as they pertain to the acquisition of gravity disturbances within the cap was omitted under the assumption that they do not differ significantly from the corresponding requirements of gravity anomaly data, as examined by Christodoulidis (1976).

The errors of primary interest, therefore, were those due to the neglect of the high-degree potential harmonic coefficients, as well as the errors in the available coefficients. A new model for the standard deviations of the coefficients

was introduced to better simulate their accuracy when they are determined from terrestrial gravity data. The final analysis was based on an assumed set of potential coefficients to degree 180 and on various cap radii between 0° and 30°. Furthermore, the analysis was expanded to include investigations with respect to the conventional formulation of point and mean undulations; that is, in terms of gravity anomalies within the cap plus potential coefficients.

Figures 2 through 5 demonstrate that as the distance between the points of computation increases, so do the commission errors (due to erroneous potential coefficients) for all values of the cap radius, as well as $\bar{n}$, the maximum degree of the coefficients. However, for large values of $\bar{n}$ (e.g. $\bar{n} = 180$), the truncation error is essentially independent of the separation between the points. Naturally, both the commission and truncation errors increase with a decrease in the cap size because the undulations must then rely more heavily on the potential coefficients.

A comparison of errors derived through Methods A and B (see (56)) showed that Method B, for the most part, is not inferior to Method A, and in some cases it may yield as much as a 30% improvement in accuracy (cf. the curves in Figure 7: for $\psi_{PQ} = 1500$ km, $\epsilon_{\Delta g} = 10$ mgal (1 mgal), Method A gives 48 cm (8 cm) and Method B gives 33 cm (5 cm)). For small spherical caps ($\psi_o < 2^\circ$), the two methods give practically equivalent error estimates (Figure 7: the error for $\psi_o = 2^\circ$, $\psi_{PQ} = 1500$ km, $\epsilon_{\Delta g} = 10$ mgal (1 mgal) is about 75 cm (13 cm); with a maximum error (at $\psi_o = 0^\circ$) in undulation differences of 151 cm (68 cm)). The confidence that can be placed on either method taken individually depends on how realistic the models are for the degree variances of gravity anomalies and potential coefficient errors. For example, the truncation error can vary 30% to 40% by changing the degree variance model c_n (see Table 3). (However this may be of little consequence to the total error when $\bar{n}$ is large, for then the truncation error is often smaller than the commission error.)

As mentioned in section 1, the possibility of determining oceanic geoid undulations from an integral of gravity disturbances, thus dispensing with reductions to the geoid, prompted the investigation of Method B. In contrast, Method A is predicated on the availability of gravity anomalies reduced to the geoid, this being a feasible hypothesis if the sea surface topography is known beforehand, perhaps through an oceanographic model (or if the error caused by neglecting it can be tolerated). For small caps, when both methods of computing undulations render similar errors, the route to follow may be decided by weighing the problem of acquiring such sea surface topography against the need for altimeter measurements which are required for the computation of gravity disturbances. The latter requirement demands considerations with respect to the accuracy of the radial positional component of a satellite-borne altimeter (and the accuracy of the altimetry itself). For example, in view of the radial component of the gradient of normal gravity ($\approx .31$ mgal/m), the sea surface height above the ellipsoid should be known (from altimetry, see Figure 1) to better than 3 m in order to derive gravity disturbances with an accuracy greater than 1 mgal (this

being required for data within the cap if the potential coefficients for the outer zone contribution are determined from mean anomalies accurate to 1 mgal: see section 7).

For larger caps ($\psi_0 = 5°$ to $30°$), the apparent improvement in the truncation and commission errors according to Method B may constitute an additional factor to consider when choosing the particular method of computing undulations. Quite significant reductions in the error, as compared to Method A, are found for large caps when the zero- and first-degree harmonics of the gravity disturbances do not exist (or are known) (and this may be the more appropriate premise on which to base comparisons to Method A). Appendix C includes an abbreviated analysis of errors derived through the modified kernel function $\bar{S}^*(\psi)$ (see section 3). It is shown there that for $\psi_0 = 30°$ and small separations ψ_{PQ}, the reduction in error (from Method A to Method B, modified) is 75% to 90%, and for $\psi_0 = 10°$, it is as much as 50%. For larger separations ($\psi_{PQ} > 1000$ km), the difference between Method A and Method B (modified) is substantial (about 50%) only if the truncation error is the predominant error source (e.g. if $\epsilon_{\Delta g} =$ 1 mgal). On the other hand, as ψ_{PQ} increases, the difference between Method B and Method B (modified) becomes less conspicuous. In the comparisons above, it is assumed that the gravity data within the cap is perfect and continuous. The reader is referred to the table of Appendix C for specific values of the estimated RMS errors.

Finally, in regard to mean undulation differences, it was seen that the estimated errors are substantially reduced only when the truncation error is the dominating constituent. In the latter case, a typical reduction of 50% (from 68 cm to 31 cm, for $\epsilon_{\Delta g} = 1$ mgal) is attained when potential coefficients to degree 180 are used to compute $1° \times 1°$ mean undulation differences instead of corresponding point values.

Taking all numerical comparisons into consideration, it is apparent that for small caps ($\psi_0 < 10°$) the stringency of the data requirements as estimated by Christodoulidis (1976) for a 10 cm relative oceanic geoid has not diminished significantly in the case when undulations are determined on the basis of gravity disturbances. For larger caps, some improvement in the truncation and commission errors is indicated, but whether sufficiently dense and accurate gravity data can be amassed within large caps (say, with radius $\psi_0 = 20°$ or $30°$) is questionable at present.

References

Christodoulidis, D. C., "On the Realization of a 10 cm Relative Oceanic Geoid," Report No. 247, Department of Geodetic Science, The Ohio State University, Nov. 1976.

Colombo, O., "Optimal Kernels for Band-Limited Data," Unisurv G-27, Department of Geodesy, University of New South Wales, 1977.

DeWitte, L., "Truncation Errors in the Stokes and Vening Meinesz Formulae for Different Order Spherical Harmonic Gravity Terms," Aerospace Report No. TR-669 (S6230-37)-5, San Bernardino Operations Aerospace Corporation, San Bernardino, California, Sept. 20, 1966.

Hagiwara, Y., "A New Formula for Evaluating the truncation error coefficient," Bulletin Géodésique, vol. 50, pp. 131-135, 1976.

Heiskanen, W. A. and H. Moritz, Physical Geodesy, W.H. Freeman and Co., San Francisco, 1967.

Hotine, M., Mathematical Geodesy, ESSA Monograph No. 2, U.S. Department of Commerce, Washington, D.C., 1969.

Jekeli, C., "An Investigation of Two models for the degree variances of global covariance functions," Report No. 275, Department of Geodetic Science, The Ohio State University, Sept. 1978.

Meissl, P., "A Study of Covariance functions related to the earth's disturbing Potential," Report No. 151, Department of Geodetic Science, The Ohio State University, April 1971.

Molodenskii, M. S., et al., Methods for the Study of the External Gravitational Field and Figure of the Earth, translated from Russian (1960), Israel Program for Scientific Transactions, Jerusalem, 1969.

Moritz, H., "Advanced Least-Squares Methods," Report No. 175, Department of Geodetic Science, The Ohio State University, June 1972.

Moritz, H., "Precise Gravimetric Geodesy," Report No. 219, Department of Geodetic Science, The Ohio State University, June 1974.

Moritz, H., "Covariance functions in least-squares collocation," Report No. 240, Department of Geodetic Science, The Ohio State University, June 1976.

Moritz, H., "Statistical Foundations of Collocation," Report No. 272, Department of Geodetic Science, The Ohio State University, June 1978.

Paul, M. K., "A method of evaluating the truncation error coefficient for geoidal height," Bulletin Géodésique, No. 110, pp. 413-425, 1973.

Rapp, R. H., "Analytical and numerical differences between two methods for the combination of gravimetric and satellite data," Bolletino D. Geophysica Teorica Ed. Applicata, Vol. 11, pp. 108-118, 1969.

Rapp, R. H., "Accuracy of Geoid Undulation Computations," Journal of Geophysical Research, Vol. 78, No. 32, pp. 7589-7595, Nov. 10, 1973.

Rapp, R. H., "A Global 1° x 1° anomaly field combining satellite, Geos-3 altimeter and terrestrial anomaly data," Report No. 278, Department of Geodetic Science, The Ohio State University, Sept. 1978.

Rapp, R. H. and R. Rummel, "Methods for the Computation of Detailed Geoids and their Accuracy," Report No. 233, Department of Geodetic Science, The Ohio State University, Nov. 1975.

Sjöberg, L., "The Accuracy of Geoid Undulations by Degree Implied by Mean Gravity Anomalies on a Sphere," Journal of Geophysical Research, in press, 1979.

Tscherning, C. and R. H. Rapp, "Closed covariance expressions for the gravity anomalies, geoid undulations, and deflections of the vertical implied by anomaly degree variance models," Report No. 208, Department of Geodetic Science, The Ohio State University, May 1974.

Appendix A

The integration of

$$\overline{Q}_n(\psi_o) = \int_{\psi_o}^{\pi} \overline{S}(\psi)\, P_n(\cos\psi)\, \sin\psi\, d\psi, \quad \psi_o \neq 0$$

is achieved by utilizing the recurrence relations of Legendre polynomials. Let $P_n(x)$ (or simply P_n) denote the n^{th}-degree Legendre polynomial and let $P_n'(x)$ (or simply P_n') denote its derivative with respect to the argument x. The following recurrence formulas are well known:

$$(n+1)\, P_{n+1} + n P_{n-1} = (2n+1)\, x\, P_n \tag{A.1}$$

$$(1-x^2)\, P_n' = n\,(P_{n-1} - x P_n) \tag{A.2}$$

$$(2n+1)\, P_n = P_{n+1}' - P_{n-1}' \tag{A.3}$$

To facilitate the integration, let $t = \cos\psi$ and $x = \cos\psi_o$. Then the function $\overline{S}(\psi)$ (see equation (4)) becomes

$$\overline{S}(t) = \sqrt{\frac{2}{1-t}} - \ell n\left(1+\sqrt{\frac{2}{1-t}}\right), \quad t \neq 1 \tag{A.4}$$

and

$$\overline{Q}_n(x) = \int_{-1}^{x} \sqrt{\frac{2}{1-t}}\, P_n(t)\, dt - \int_{-1}^{x} P_n(t)\, \ell n\left(1+\sqrt{\frac{2}{1-t}}\right) dt, \quad x \neq 1 \tag{A.5}$$

In all further derivations, it will be understood that $x \neq 1$. For $n \geq 0$,

let $$L_n(x) = \frac{1}{\sqrt{2}} \int_{-1}^{x} \frac{P_n(t)\, dt}{\sqrt{1-t}}, \quad K_n(x) = \frac{1}{2\sqrt{2}} \int_{-1}^{x} \frac{P_n(t)}{(1-t)^{3/2}}\, dt$$

and for $n \geq 1$, $$I_n(x) = \int_{-1}^{x} P_n(t)\, dt = \frac{1}{2n+1}\left(P_{n+1}(x) - P_{n-1}(x)\right) \tag{A.6}$$

The last equality follows from equation (A.3) and the fact that

$$P_n(-1) = (-1)^n, \quad \text{for all } n \geq 0 \tag{A.7}$$

Hagiwara (1976) shows that

$$K_{n+1} - 2K_n + K_{n-1} = \frac{-1}{\sqrt{2(1-x)}}\, I_n, \quad n > 1$$

$$\text{with} \quad K_o = -\frac{1}{2}\left(1 - \sqrt{\frac{2}{1-x}}\right), \quad K_1 = K_o - \left(1 - \sqrt{\frac{1-x}{2}}\right) \tag{A.8}$$

$$\text{and*} \quad L_n = \frac{I_n}{\sqrt{2(1-x)}} - \left[K_{n+1} - K_{n-1}\right] \frac{1}{2n+1}, \quad n \geq 1 \tag{A.9}$$

* This differs from the misprinted version in Hagiwara's paper.

The first integral in (A.5) is

$$\int_{-1}^{x} \sqrt{\frac{2}{1-t}}\, P_n(t)\, dt = 2 L_n(x) \tag{A.10}$$

Let the second integral in (A.5) be

$$R_n(x) = -\int_{-1}^{x} P_n(t)\, \ell n \left(1 + \sqrt{\frac{2}{1-t}}\right) dt \tag{A.11}$$

Substituting the recurrence formula (A.1) gives

$$R_n(x) = -\frac{n-1}{n} R_{n-2}(x) - \frac{2n-1}{n}\int_{-1}^{x} t P_{n-1}(t)\, \ell n \left(1 + \sqrt{\frac{2}{1-t}}\right) dt \tag{A.12}$$

Now, putting (A.2) in the integral of (A.12) results in

$$\begin{aligned} R_n(x) &= -\frac{n-1}{n} R_{n-2}(x) - \frac{2n-1}{n}\int_{-1}^{x}\left[P_{n-2}(t)\, \ell n \left(1+\sqrt{\frac{2}{1-t}}\right) + \right. \\ &\quad \left. -\frac{1}{n-1}(1-t^2) P'_{n-1}(t)\, \ell n \left(1+\sqrt{\frac{2}{1-t}}\right)\right] dt \\ &= R_{n-2}(x) + \frac{2n-1}{n(n-1)}\int_{-1}^{x}(1-t^2) P'_{n-1}(t)\, \ell n \left(1+\sqrt{\frac{2}{1-t}}\right) dt \end{aligned} \tag{A.13}$$

The integral in (A.13) is integrated by parts. To this end, let

$$w = (1-t^2)\, \ell n \left(1+\sqrt{\frac{2}{1-t}}\right)$$

After some simplifications, it is found that

$$dw = \left[-\sqrt{\frac{1-t}{2}} + 1 - 2t\, \ell n \left(1+\sqrt{\frac{2}{1-t}}\right)\right] dt$$

Also, if $dv = P'_{n-1}(t)\, dt$, then $v = P_{n-1}(t)$ and the integral in (A.13) becomes

$$\begin{aligned} \int_{-1}^{x} w\, dv &= w v \Big|_{-1}^{x} - \int_{-1}^{x} v\, dw \\ &= (1-x^2)\, \ell n \left(1+\sqrt{\frac{2}{1-x}}\right) P_{n-1}(x) + \frac{1}{\sqrt{2}}\int_{-1}^{x}\sqrt{1-t}\, P_{n-1}(t)\, dt + \\ &\quad - \int_{-1}^{x} P_{n-1}(t)\, dt + 2\int_{-1}^{x} P_{n-1}(x)\, t\, \ell n \left(1+\sqrt{\frac{2}{1-t}}\right) dt \end{aligned}$$

Substituting this back into (A.13) yields

$$\begin{aligned} R_n(x) &= R_{n-2}(x) + \frac{2n-1}{n(n-1)}(1-x^2)\, \ell n \left(1+\sqrt{\frac{2}{1-x}}\right) P_{n-1}(x) + \\ &\quad + \frac{2n-1}{\sqrt{2}(n-1)n} A_{n-1}(x) - \frac{2n-1}{n(n-1)} I_{n-1}(x) + 2\frac{2n-1}{n(n-1)} B_{n-1}(x) \end{aligned} \tag{A.14}$$

$I_{n-1}(x)$ is given by (A.6), and

$$A_{n-1}(x) = \int_{-1}^{x} \sqrt{1-t}\, P_{n-1}(t)\, dt,$$

$$B_{n-1}(x) = \int_{-1}^{x} t\, P_{n-1}(t)\, \ell n \left(1+\sqrt{\frac{2}{1-t}}\right) dt$$

$A_{n-1}(x)$ is computed by inserting (A.3) and integrating by parts:

$$A_{n-1}(x) = \frac{1}{2n-1}\left[\sqrt{1-x}\,(P_n(x) - P_{n-2}(x)) - \sqrt{2}\,(P_n(-1) - P_{n-2}(-1)) + \right.$$

$$\left. + \frac{1}{\sqrt{2}}\,(L_n(x) - L_{n-2}(x))\right] \qquad (A.15)$$

The second term in (A.15) is zero in view of (A.7) and $L_n(x)$ is given by (A.6). Finally, $B_{n-1}(x)$ is obtained by substituting (A.1):

$$B_{n-1}(x) = -\frac{n}{2n-1}\,R_n(x) - \frac{n-1}{2n-1}\,R_{n-2}(x) \qquad (A.16)$$

Also, from (A.6) we find

$$I_{n-1}(x) = \frac{1}{2n-1}\,(P_n(x) - P_{n-2}(x)) \qquad (A.17)$$

Putting (A.15), (A.16), and (A.17) into (A.14), it is readily found that

$$\frac{n+1}{n-1}\,R_n(x) = \frac{n-2}{n}R_{n-2}(x) + \frac{1}{2n(n-1)}\,(L_n(x) - L_{n-2}(x)) +$$

$$+ \frac{1}{n(n-1)\sqrt{2}}\,(\sqrt{1-x} - \sqrt{2})\,(P_n(x) - P_{n-2}(x)) +$$

$$+ \frac{2n-1}{n(n-1)}\,\ell n \left(1+\sqrt{\frac{2}{1-x}}\right)\left(1-x^2\right) P_{n-1}(x) \qquad (A.18)$$

The remaining problem is to find a suitable recursive relation for the $L_n(x)$ functions. This can be done with some juggling of equations (A.8) and (A.9). For convenience, let $u = 1/\sqrt{2(1-x)}$, then

(A.8) becomes $K_{n+1} - 2K_n + K_{n-1} = -u\, I_n$ (A.19)

and (A.9) becomes $L_n = u\, I_n - (K_{n+1} - K_{n-1})\frac{1}{2n+1}$ (A.20)

Solving (A.19) for K_{n+1} and substituting into (A.20) yields

$$(2n+1)\,L_n = (2n+2)\,u\,I_n - 2K_n + 2K_{n-1}$$

Also, $(2n+3)\,L_{n+1} = (2n+4)\,u\,I_{n+1} - 2K_{n+1} + 2K_n$

Adding these last two identities and substituting (A.20) gives

$$(2n+3)\,L_{n+1} = 2u\,[(n+2)\,I_{n+1} - n\,I_n] + (2n+1)\,L_n$$

Or, finally

$$(2n+1)\,L_n(x) = \sqrt{\frac{2}{1-x}}\,[(n+1)\,I_n(x) - (n-1)\,I_{n-1}(x)] + \\ + (2n-1)\,L_{n-1}(x), \qquad n \geq 1$$

$$\text{with } L_0(x) = 2 - 2\sqrt{\frac{1-x}{2}} \tag{A.21}$$

$L_0(x)$ is easily determined from (A.6). The starting functions $R_0(x)$ and $R_1(x)$ are found by integrating (A.11) directly, changing the variable t to

$$t = 1 - 2z^2, \qquad z \neq 0$$

and integrating by parts. Only the final results are stated below.

The recursive formulation of $\bar{Q}_n$ may be summarized as follows:

For $x = \cos\psi_0$, $\psi_0 \neq 0$:

$$\bar{Q}_n(x) = 2\,L_n(x) + R_n(x), \qquad n \geq 0$$

$$\text{where } (2n+1)\,L_n(x) = \sqrt{\frac{2}{1-x}}\,[(n+1)\,I_n(x) - (n-1)\,I_{n-1}(x)] + \\ + (2n-1)\,L_{n-1}(x), \qquad n \geq 1$$

$$\text{with } L_0 = 2 - 2\sqrt{\frac{1-x}{2}}$$

$$\text{and } I_n(x) = \frac{1}{2n+1}\,[P_{n+1}(x) - P_{n-1}(x)], \qquad n \geq 1$$

$$\text{and } (n+1)\,R_n(x) = \frac{1}{n}(n-1)(n-2)\,R_{n-2}(x) + \frac{1}{2n}[L_n(x) - L_{n-2}(x)] + \\ + \frac{2n-1}{n}\left[\sqrt{\frac{1-x}{2}} - 1\right] I_{n-1}(x) + \\ + \frac{2n-1}{n}(1-x^2)\,P_{n-1}(x)\,\ell n\left(1+\sqrt{\frac{2}{1-x}}\right), \qquad n \geq 2$$

$$\text{with } R_0(x) = -2\,\ell n\left(1+\sqrt{\frac{1-x}{2}}\right) + (1-x)\,\ell n\left(1+\sqrt{\frac{2}{1-x}}\right) - 2\left(1-\sqrt{\frac{1-x}{2}}\right)$$

$$\text{and } R_1(x) = \left(1-\frac{1-x}{2}\right)\left[(1-x)\,\ell n\left(1+\sqrt{\frac{2}{1-x}}\right) - 1\right] + \frac{2}{3}\left(1-\frac{1-x}{2}\sqrt{\frac{1-x}{2}}\right)$$

$$\text{and } (n+1)\,P_{n+1}(x) + n\,P_{n-1}(x) = (2n+1)\,x\,P_n(x), \qquad n > 2$$

$$\text{with } P_0(x) = 1$$

$$\text{and } P_1(x) = x$$

Appendix B. Concerning the factor σ^n in equation (46)

The extension of the disturbing potential into the space outside a sphere of radius R_B is given by (cf. equation (17))

$$T(r,\theta,\lambda) = \frac{kM}{R_B}\sum_{n=0}^{\infty}\left(\frac{R_B}{r}\right)^{n+1}\sum_{m=0}^{n}(\bar{C}_{nm}\cos m\lambda + \bar{S}_{nm}\sin m\lambda)\,\bar{P}_{nm}(\cos\theta)$$

$$= \sum_{n=0}^{\infty} T_n\left(\frac{R_B}{r}\right)^{n+1} \qquad (B.1)$$

where $\bar{C}_{nm}$, $\bar{S}_{nm}$ refer to this sphere (that is, R is replaced by R_B in equation (17)). On the sphere of radius $R > R_B$, it is

$$T(R,\theta,\lambda) = \sum_{n=0}^{\infty} T_n\left(\frac{R_B}{R}\right)^{n+1} = \sum_{n=0}^{\infty}\tilde{T}_n \qquad (B.2)$$

If N_2 is computed on the sphere of radius R, then according to equation (16) it is

$$N_2 = \frac{R}{2\gamma}\sum_{n=0}^{\infty}\bar{Q}_n\,\tilde{\delta g}_n\,, \qquad \gamma = \frac{kM}{R^2} \qquad (B.3)$$

where $\tilde{\delta g}_n$ on this sphere is obtained from (18) and (B.2):

$$\tilde{\delta g}_n = \frac{n+1}{R}\,\tilde{T}_n = \frac{n+1}{R}\,T_n\left(\frac{R_B}{R}\right)^{n+1} \qquad (B.4)$$

Consequently, the substitution of (B.4) and T_n of (B.1) into (B.3) leads to

$$N_2 = \frac{R}{2}\sum_{n=0}^{\infty}(n+1)\,\bar{Q}_n\left(\frac{R_B}{R}\right)^n\sum_{m=0}^{n}(\bar{C}_{nm}\cos m\lambda + \bar{S}_{nm}\sin m\lambda)\,\bar{P}_{nm}(\cos\theta)$$

The corresponding formulation of the error ϵ_1 differs from equation (38) by the factors $(R_B/R)^n$; this implies that the degree variances ξ_n as given by (40) should be modified by the factor $\sigma^n = (R_B^2/R^2)^n$.

Appendix C. Truncation Coefficients Implied by the Kernel Function $\bar{S}^*(\psi) = \bar{S}(\psi) - 1 - \frac{3}{2}\cos\psi$

If the series expansion of the gravity disturbance function δg (equation (14)) contains no zero- and first-degree terms, then the integral equation (5) becomes

$$N = \frac{R}{4\pi\gamma}\iint_{\sigma}\sum_{n=2}^{\infty}\delta g_n\sum_{\ell=2}^{\infty}\frac{2\ell+1}{\ell+1}\,P_\ell(\cos\psi)\,d\sigma \qquad (C.1)$$

where the series expansion for $\bar{S}(\psi)$ (equation (4)) has been used and $P_\ell(\cos\psi)$, $\ell = 0, 1$ are excluded because they are orthogonal to the harmonic functions of δg. Equivalently, equation (C.1) is

$$N = \frac{R}{4\pi\gamma}\iint_{\sigma}\delta g\;\bar{S}^*(\psi)\,d\sigma \qquad (C.2)$$

where $\bar{S}^*(\psi) = \bar{S}(\psi) - 1 - \frac{3}{2}\cos\psi$. This modified kernel function defines the following truncation coefficients (cf. equation (11))

$$\bar{Q}_n^* = \int_{\psi_o}^{\pi} \bar{S}^*(\psi)\, P_n(\cos\psi)\, \sin\psi\, d\psi \qquad (C.3)$$

$$= \bar{Q}_n - \int_{\psi_o}^{\pi} (1 + \tfrac{3}{2}\cos\psi)\, P_n(\cos\psi) \sin\psi\, d\psi \qquad (C.4)$$

It is noted that for $\psi_o = 0$, $\bar{Q}_n^* = \bar{Q}_n$, $n \geq 2$; also $\bar{Q}_o^*$ and $\bar{Q}_1^*$ are <u>not</u> equal to zero unless $\psi_o = 0$, but this is immaterial in the error formulas since $\delta g_o = 0 = \delta g_1$.

The integral in equation (C.4) is evaluated by utilizing the results of Appendix A (let $t = \cos\psi$, $x = \cos\psi_o$).

$$\int_{\psi_o}^{\pi} P_n(\cos\psi)\, \sin\psi\, d\psi = I_n(x) \qquad (C.5)$$

$$\int_{\psi_o}^{\pi} \cos\psi\, P_n(\cos\psi)\, \sin\psi\, d\psi = \int_{-1}^{x} t\, P_n(t)\, dt \qquad (C.6)$$

The integral in (C.6) is directly integrable when the recursion formula (A.1) is introduced:

$$\int_{-1}^{x} t\, P_n(t)\, dt = \frac{1}{2n+1} \int_{-1}^{x} ((n+1)\, P_{n+1}(t) + n\, P_{n-1}(t))\, dt$$

$$= \frac{n+1}{2n+1}\, I_{n+1}(x) + \frac{n}{2n+1}\, I_{n-1}(x) \qquad (C.7)$$

Substituting (C.5) and (C.7) into (C.4),

$$\bar{Q}_n^* = \bar{Q}_n - [\, I_n + \frac{3}{4n+2} (\, (n+1)\, I_{n+1} + n\, I_{n-1}\,)\,]$$

where $\bar{Q}_n$ and I_n are given on page 38.

The equation for the global error estimates m_1 and m_2 of the outer zone undulation differences are obtained by replacing $\bar{Q}_n$ with $\bar{Q}_n^*$ in equations (46) and (36). The following table indicates the type of corresponding reductions that can be expected in the error estimates.

Total (RMS) errors (cm) in undulation differences assuming perfect and continuous gravity data within a cap of radius ψ_o ($\bar{n} = 180$, Method B, parenthetical values are obtained via Method A).

		$\epsilon_{\Delta g} = 1$ mgal		$\epsilon_{\Delta g} = 10$ mgal	
	ψ_{PQ} [km]	using $\bar{Q}_n$ (Q_n)	using $\bar{Q}_n^*$	using $\bar{Q}_n$ (Q_n)	using $\bar{Q}_n^*$
$\psi_o = 10°$	100	4.8 (7.4)	3.5	8.2 (12.4)	6.0
	1000	5.0 (7.6)	3.8	27.3 (39.5)	23.0
	2000	5.7 (8.6)	4.7	37.9 (54.8)	36.0
$\psi_o = 30°$	100	2.1 (1.7)	0.1	3.6 (3.1)	0.8
	1000	2.3 (2.1)	0.8	12.9 (14.5)	8.3
	2000	2.6 (2.9)	1.6	18.7 (25.0)	16.2

Generally, for most n, $\bar{Q}_n^*$ is less in magnitude than $\bar{Q}_n$, and the absolute differences between these coefficients increase substantially as the radius ψ_o of the cap changes from 10° to 30°. The truncation error ($\bar{n} = 180$) for $\psi_o = 30°$ is practically nonexistent (≈ 0.02 cm, compared to 1.9 cm when $\bar{Q}_n$ is used); while for $\psi_o = 10°$, the truncation error of 3 cm to 4 cm is closer to the 4 cm to 5 cm that is obtained with $\bar{Q}_n$. This accounts for the considerable decreases in error for the larger cap, particularly when ψ_{PQ} is small as the commission error is then minimal. The tabulated values which are enclosed in parentheses correspond to error estimates based on Method A (using the coefficients Q_n). Note that both Q_n and $\bar{Q}_n^*$ are derived from kernel functions ($S(\psi)$ and $\bar{S}^*(\psi)$, respectively) whose zero- and first-degree harmonic coefficients are zero.

We see then the noticeable improvement (up to 50% for $\psi_o = 10°$) in the accuracy of geoid undulation differences when determined on the basis of perfect and continuous gravity disturbance data within a cap of radius $\psi_o = 30°$, and when the modified kernel function $\bar{S}^*(\psi)$ is employed. This naturally leads to further possible improvements with more discriminating selections of the kernel function, as alluded to in section 10.